國 立 交 通 大 學

機械工程研究所
碩士論文

機載雷達偵照系統之視線控制

Line-of-Sight Control in Airborne Radar Reconnaissance

System

研 究 生： 張淦垚

指導教授： 成維華 教授

中華民國九十五年六月

機載雷達偵照系統之視線控制

Line-of-Sight Control in Airborne Radar Reconnaissance System

研 究 生：張淦垚　　　　　　　　　Student：Kan-Yao Chang

指導教授：成維華　　　　　　　　　Advisor：Wei-Hua Chieng

國 立 交 通 大 學

機 械 工 程 學 系

碩 士 論 文

A Thesis
Submitted to Institute of Mechanical Engineering
College of Engineering
National Chiao Tung University
in partial Fulfillment of the Requirements
for the Degree of
Master
in

Mechanical Engineering

June 2006
Hsinchu, Taiwan, Republic of China

中華民國九十五年六月

機載雷達偵照系統之視線控制

研究生：張淦垚　　　　　　　　　　　　指導教授：成維華 教授

國立交通大學機械工程學系研究所

摘　　　要

　　雷達是利用反射波來偵測遠方目標物並獲得其方位的一種裝置。機載雷達由於飛機載具本身的運動、受到大氣亂流的干擾或飛機本身結構的震動等，造成雷達掃瞄軌跡的偏移，致使雷達搜索性能降低。為了改善此一現象，雷達必須針對飛機運動的變化修正雷達掃瞄路徑軌跡，以消除其運動誤差。本論文主旨在於實現機載雷達天線穩定系統，於雷達天線基座上加裝一個可作兩軸旋轉之環架式機構，利用此機構補償飛機姿態的變化，使天線視線能夠固定對著某一方位。在此系統中，藉由視線控制的演算法產生穩定天線所需的命令，並利用陀螺儀及角度感測器作為回授訊號之感測器，進而設計控制器以降低追蹤誤差。

Line-of-Sight Control in Airborne Radar Reconnaissance System

Student：Kan-Yao Chang   Advisor：Dr. Wei-Hua Chieng

Institute of Mechanical Engineering
National Chiao Tung University

Abstract

Radar is a device of using electromagnetic waves to detect the presence of the target and extract its location and relative velocity. The airborne radar deviates from its predicted trajectory by pilot-induced maneuvers, atmospheric gusts disturbance and structural vibrations, and will decrease the detection efficiency of radar. In order to improve the problem, we have to compensate the motion uncertainty of aircraft and correct the motion deviation of radar. The purpose of the thesis is to implement the antenna stabilization system of airborne radar. By setting up a two-axis gimbal mechanism on the antenna pedestal, we can compensate the changing attitudes of aircraft and stabilize the antenna line-of-sight in a designated earth-fixed location. Algorithm used for line-of-sight control generates commands to stabilize and point antenna. The gyroscope and encoders are taken as the sensors of feedback signals in this system. PID controller is developed to minimize tracking error and improve system performance.

Acknowledgement

I would like to deeply appreciate my advisor Prof. Wei-Hua Chieng for his guidance during my graduate study. I would also want to thank for my seniors, Yong-Chieng Tong, Chia-Feng Yang and Bing-Ling Wu. They taught me a lot of knowledge in my research.

Contents

List of Figures

List of Tables

Chapter 1 Introduction

1.1 Motives and Objectives

Radar is derived from radio detection and ranging. It is a method of using electromagnetic waves to remote-sense the position, velocity, and identifying characteristics of targets. This is accomplished by illuminating a volume of space with electromagnetic energy and sensing the energy reflected by objects in that space. In the airborne radar reconnaissance system, imaging radar provides all-weather, day and night, high resolution imagery of ground targets for joint armed forces users. The imaging function is essentially used in military applications for intelligence, surveillance, reconnaissance, and navigation.

However, when a radar is installed on board an aircraft with velocity and has roll, pitch, or yaw motion, the change of aircraft attitude in the inertial space make antenna could not receive reflected waves precisely to detect targets and measure their ranges and directions. Aircraft motion errors will cause defocusing, thus degrade the resolution of image. The effect of very low frequency motion is to cause geometric distortion and poor map accuracy; higher frequency motion causes distortion of radar image; i.e. degradation of sidelobes, and resolution loss.

In order to minimize the influences induced by aircraft motion, motion compensation is necessary. Motion compensation refers to corrections for any change in the velocity vector caused by either atmosphere disturbances or intentional maneuvering. It is classified into signal-based and sensor-based. In the signal-based motion compensation, many signal processing algorithms are developed to estimate the phase error of receiving microwave signal, like PGA

and SPGA etc. In the thesis what we discuss is sensor-based motion compensation. The objective is to design and implement an airborne antenna stabilization system. The system is composed of a series of D.C. servomotors and antenna gimbal mechanism in conjunction with inertial measurement sensors. It can work actively to maintain the antenna inertial attitude while antenna transmitting electromagnetic waves and receiving reflected waves. The servomechanism stabilizes the antenna pointing angle such that the system can continuously point the antenna at the desired position in the space regardless of aircraft motion.

1.2 Research Orientation

The primary purpose of this research is to point and stabilize the line-of-sight of radar antenna that is mounted on the underside of a high altitude unmanned reconnaissance aircraft to provide all-weather high resolution imagery of ground targets. The major work is to accomplish a real-time antenna stabilization system.

Algorithm used for line-of-sight control is developed to command the antenna line-of-sight with respect to a local level reference frame that is decoupled from aircraft angular motion. The algorithm generates inertial rate and gimbal angle commands, where the inertial rate loops can control the antenna earth-fixed rates while a map is made, and the position loops can remove gyro drift and servo position biases accumulated during the scan bar. Line-of-sight scan commands are generated to ensure that the antenna line-of-sight be stabilized regardless of aircraft motion and its earth projections result in gap-free coverage. The commands are continually updated according to the real-time computations.

A gimbal mechanism equipped two D.C. servomotors is built up to stabilize antenna line-of-sight. The gimbal mechanism can do two-axis rotation, which are azimuth and elevation. The antenna is fitted with the roll-stabilizing system, followed by the servo-loop in azimuth carrying an elevation servomechanism to direct line-of-sight to designated earth-fixed locations. Gyroscope and encoders are primary sensors in the system. Gyroscope measures the changing attitudes of aircraft which are absolute roll, pitch, and yaw angles. Host computer continuously receives these data and generates correct compensated angles to drive servomotors after a series of complicated calculations. Encoders are coupled to the motor shafts, to provide feedback signals for the position feedback loops closed around the antenna drives. In the system, PID Controller is adopted to reduce steady-state error to zero and transient state response can be appropriate adjustment. Referring to Ziegler and Nichols tuning method, PID controller parameters can be tuning to provide acceptable closed-loop response. Finally, the system is under different frequency disturbance to simulate the antenna stabilization system working on the aircraft.

This thesis describes the salient features of the antenna stabilization system design with emphasis on the algorithm used for line-of-sight control, command generation, system design and performance analysis. Experiment results will be presented to support the design.

Chapter 2 Line-of-Sight Control

Radar is a system that transmits an electromagnetic wave in a given direction and then detects this same wave reflected back by an obstacle in its path. Antenna Line-of-Sight (LOS) deviates from its predicted direction during radar operation by pilot-induced maneuvers, atmospheric gusts disturbance and structural vibrations, and will smear the high-resolution images. Figure 2.1 shows the relationship between LOS and tracking line.

With a high-performance stabilizer is used, which absorbs the vibrations of the aircraft and stabilizes the antenna LOS, the resulting original images have very little waving and blurring, leading to fewer problems for post-processing. The stabilizer's effect on image quality for linear scan applications is shown in Figure 2.2[13]. The fine stabilization is jointly achieved with two-axis gimbal servomechanism mounted on the aircraft. The radar antenna subassembly is mounted on the inner gimbal that directs the antenna LOS to designated earth-fixed direction. An on-gimbal inertial rate sensor provides the 2 degree-of-freedom inertial reference to stabilize the antenna LOS. A series of coordinate transformations will be applied to generate gimbal commands.

2.1 Kinematics

2.1.1 Coordinate Transformations[8]

The Coordinate transformation describing the relation between one coordinate and the next has been called a **C** matrix. A **C** matrix is simply a homogeneous transformation describing the relative translation and rotation

between two coordinate systems. $\mathbf{C_1}$ describes the position and orientation of the first coordinate system. $\mathbf{C_2}$ describes the position and orientation of the second coordinate system with respect to the first. Thus the position and orientation of the second coordinate system in base coordinates are given by the matrix product

$$\mathbf{T_2} = \mathbf{C_1\,C_2} \qquad\qquad (2\text{-}1)$$

Similarly, $\mathbf{A_3}$ describes the third coordinate system in terms of the second

$$\mathbf{T_3} = \mathbf{C_1\,C_2\,C_3} \qquad\qquad (2\text{-}2)$$

And so on. These products of $\mathbf{C}$ matrices have historically been called $\mathbf{T}$ matrices, with the leading superscript omitted if it is 0.

In general, if we post-multiply a transform representing a frame by a second transformation describing a rotation and/or translation, we make that translation and/or rotation with respect to the frame axes described by the first transformation. If we pre-multiply the frame transformation by a transformation representing a translation and/or rotation, then that translation and/or rotation is made with respect to the base reference coordinate frame.

2.1.2 Translational Mapping[9]

In Figure 2.3, a position defined by the vector ^{B}P. We wish to express this point P in space in terms of the coordinate system $\{A\}$, when $\{A\}$ has the same orientation as the coordinate system $\{B\}$. $\{B\}$ differs from $\{A\}$ only by a translation which is given by $^{A}O_B$. The description of point P relative to $\{A\}$, ^{A}P can be calculated, by vector addition
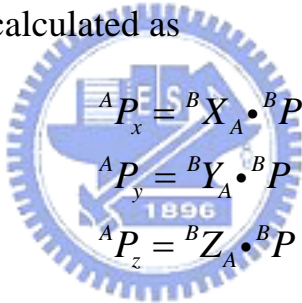
$$^{A}P = {}^{A}P + {}^{A}O_B \qquad\qquad (2\text{-}3)$$

2.1.3 Rotational Mapping[9]

At first, the unit vectors on the three principal axes of the coordinate system {A} in terms of the coordinate system {B} are ^BX_A, ^BY_A, ^BZ_A. For convenience we stack the transpose of these three unit vectors together as the rows of a 3x3 matrix. This matrix will be called a rotation matrix, we name it with the notation ^BR_A. So a rotation matrix can be interpreted as follows

$$^AR_B = \begin{bmatrix} ^BX_A \\ ^BY_A \\ ^BZ_A \end{bmatrix}$$ (2-4)

In order to calculate ^AP, we note that the components of any vector are simply the projections of that vector on the unit directions of its axes. The components of ^AP may be calculated as

$$\begin{aligned} ^AP_x &= ^BX_A \bullet ^BP \\ ^AP_y &= ^BY_A \bullet ^BP \\ ^AP_z &= ^BZ_A \bullet ^BP \end{aligned}$$ (2-5)

Since we know that the row of ^BR_A are transpose of ^BX_A, ^BY_A, ^BZ_A, so ^AP can be written compactly using a rotation matrix as

$$^AP = {}^BR_A \bullet {}^BP$$ (2-6)

2.2 Operational Modes

The Wide Area Search (WAS) mode of the Unmanned Aerial Vehicles (UAV) is to fly a prescribed straight-and-level trajectory over a designated target region to record gapless imagery of potential ground targets. With the Electro-Optical (EO) sensors mounted on the underside of the aircraft, the sensor LOS is scanned about the roll gimbal axis (in scan) which is aligned with

the aircraft's roll axis. The in scan angular rates enable wide area gapless frame coverage by methodically step the LOS one Field-of-View (FOV) over the desired frame period. The orthogonal pitch gimbal axis (cross scan) is used predominantly to cancel angular rates induced by the aircraft's linear motion. The scan bar is terminated when the aircraft's induced cross scan angular motion equals one FOV frame, at which time the cross scan gimbal steps one FOV and gimbal reverses its scan to reposition the sensor LOS for scanning a subsequent scan bar in the opposite direction. The WAS mode and its geometry are illustrated in Figure 2.5 and 2.6[12].

Spotlight mode, by gradually changing the look angle of the real antenna as the radar advances and making appropriate phase corrections, the radar can repeatedly map a given region of interest. This Spotlight mode is shown in Figure 2.7, not only enables the operator to maintain surveillance over an area for an appreciable period of time but can produce maps of superior quality[15].

Stripmap mode, the central point must travel along the ground in a straight line at the speed of the aircraft. For a fully stabilized map, the central point moves along a straight line in inertial space regardless of the motion of the aircraft, see Figure 2.8. A tube of some reasonable diameter is established to allow reasonable maneuvering and yet not unduly complicate the motion compensation problem[15].

2.3 Coordinate Frames

The mathematics applied to actual missile or aircraft applications requires that we establish different coordinate system for antenna stabilization. Four principal coordinate frames are used in the command generation. Each frame is shown in Figure 2.9.

◆ Earth Centered Earth Fixed (EF) Frame – This frame is defined in WGS-84 and has its origin at the earth's geometric center. The X axis is in the equatorial plane at zero degrees longitude. Z points north through the polar axis, and Y forms an orthogonal right handed (RH) set.

◆ Local Level (LL) Frame – The frame is North-East-Down coordinate system which center is located on the aircraft body. The X axis points north direction, Y axis points east direction, and Z axis points down through earth center. Both aircraft navigation and scan take this frame as reference. The transformation from EF to LL is computed by Global Positioning System (GPS).

◆ Aircraft Body (AC) Frame – This frame has its origin at the aircraft body center. The X axis points out the nose of the aircraft and is nominally aligned with the aircraft body roll axis. Z axis points out the bottom of the aircraft and is nominally aligned with the aircraft body yaw axis. Y axis forms a RH orthogonal set and nominally points out the right wing. The transformation from LL to AC is computed by the gyroscope in the form of three attitude angles, roll, pitch and yaw, which are used by the sensor subsystem to compute the transformation matrix.

◆ Antenna LOS (S) Frame – This frame has its origin at the antenna center. It is coincident with the AC coordinate when antenna gimbal has zero azimuth and elevation gimbal angles. The antenna LOS is located at Y axis in the frame, and it points out aircraft right wing when antenna gimbal does not rotate. The transformation from AC to S is determined by two axes rotations through azimuth and elevation

gimbal angles.

In the following discussion, coordinate transforms are denoted by C_X^Y, where C is the direction cosine matrix transform from frame X to frame Y.

2.4 Command Generation[12]

A principal requirement for the command generation is to maintain the LOS position on the earth's surface at constant earth-fixed coordinates for the duration of one sensor integration period. Command generation decides the antenna gimbal commands to stabilize antenna LOS. Most of the inputs required for command generation are provided by Inertial Measurement Unit (IMU).

2.4.1 Inertial Rate Generator

The inertial rate generator analytically computes angular rate commands as a function of time to transfer the antenna LOS from an initial state to a final desired state. During scan, this is accomplished by closing the inertial rate loops to control the antenna earth-fixed rates. The inertial rate loops attenuate aircraft angular motion sensed by the on-gimbal inertial rate sensor and compensate for any unobserved angular motion induced by aircraft linear motion.

To meet coverage requirements, the sensor must be scanned with respect to an earth-fixed target at a constant rate. The mechanism for performing a slew maneuver of the LOS is described graphically in Figure 2.10. The typical maneuver requires the LOS to be repositioned from its present earth-fixed position to the next desired earth-fixed position. This problem is partitioned such that inertial rate generator analytically generates the reposition commands while the aircraft-induced rate compensation is numerically integrated.

At the inception of a transfer, two target and aircraft positions are located in EF coordinate frame. The scan is from target positon1 to target postion2 when aircraft flies a path from postion1 to positon2. To compensate for aircraft and target motion, antenna LOS inertial rate can be partitioned into two parts. $\overrightarrow{\omega_1^{ef}}$ is the angular rate assuming antenna scan from target1 to target2 and aircraft is stationary. $\overrightarrow{\omega_2^{ef}}$ is the angular rate assuming antenna scan the same point target1 and aircraft is under motion.

$$\overrightarrow{\omega_1^{ef}} = \frac{\overrightarrow{r_2} - \overrightarrow{r_1}}{\Delta T} \times \frac{1}{R}$$

$$\overrightarrow{\omega_2^{ef}} = \frac{\overrightarrow{r_{AC2}} - \overrightarrow{r_{AC1}}}{\Delta T} \times \frac{1}{R}$$

$$(2\text{-}7)$$

where $\overrightarrow{r_1}$, $\overrightarrow{r_2}$, $\overrightarrow{r_{AC1}}$ and $\overrightarrow{r_{AC2}}$ are target and aircraft position vectors represented in EF coordinates. ΔT is frame time which scan bar moves from one FOV to the next. R is length from target to aircraft.

Therefore, antenna LOS inertial rate is equated to

$$\overrightarrow{\omega_{s/ef}^{ef}} = \overrightarrow{\omega_1^{ef}} + \overrightarrow{\omega_2^{ef}} \tag{2-8}$$

$\overrightarrow{\omega_{s/ef}^{ef}}$ is comprised of three distinct rates :

$$\overrightarrow{\omega_{s/ef}^{ef}} = \overrightarrow{\omega_{S/AC}^{ef}} + \overrightarrow{\omega_{AC/LL}^{ef}} + \overrightarrow{\omega_{LL/ef}^{ef}}$$

$$\overrightarrow{\omega_{S/AC}^{ef}} = \overrightarrow{\omega_{s/ef}^{ef}} - \overrightarrow{\omega_{AC/LL}^{ef}} + \overrightarrow{\omega_{LL/ef}^{ef}}$$

$$(2\text{-}9)$$

where $\overrightarrow{\omega_{S/AC}^{ef}}$ is the angular rate of S frame with respect to AC frame, and this rate is the necessary gimbal rate command while radar mapping. $\overrightarrow{\omega_{AC/LL}^{ef}}$ is the angular rate of the aircraft with respect to LL frame, and this angular rate vector is determined from gyroscope by sensing aircraft angular velocity. $\overrightarrow{\omega_{LL/ef}^{ef}}$ is the LL frame angular rate vector with respect to the EF frame. This frame is rotated to maintain the down axis aligned with geodetic vertical. It is determined from GPS by sensing aircraft position resolved in EF coordinates.

At the conclusion of the transfer, equation (2-9) generates the appropriate antenna gimbal rate commands to control the LOS with respect to an EF frame. The LOS is at the desired earth-fixed location and rate that exactly cancels the linear and angular aircraft motion.

2.4.2 Gimbal Angle Generator

The radar antenna is servo to the unit vector by the antenna driving system. Its stabilization involves a series of coordinate rotations. The antenna LOS unit vector in antenna frame is defined by

$$\overrightarrow{u}^{S}_{LOS} = \begin{bmatrix} 0 \\ 1 \\ 0 \end{bmatrix} \qquad (2\text{-}10)$$

First, the target vector should be defined which is the direction we attempt to keep antenna toward. The target unit vector in LL frame is defined by two angles, one is azimuth and the other is elevation. The azimuth angle is called the map heading angle H_M, and it is the angle from the inertial reference north to the ground point being imaged, measured in a plane parallel to the Earth's surface. The elevation angle E_S, is measured from the horizontal plane of the aircraft to the ground point in a vertical plane. These angles are illustrated in Figure 2.11. Then the transformation from S frame to LL frame is

$$C^{LL}_{S} = Rot(z, H_m)Rot(y, E_S) \qquad (2\text{-}11)$$

where $Rot(z, H_m)$ and $Rot(y, E_S)$ are the 3x3 coordinate rotation matrices:

$$Rot(z, Hm) = \begin{bmatrix} \cos(Hm) & -\sin(Hm) & 0 \\ \sin(Hm) & \cos(Hm) & 0 \\ 0 & 0 & 1 \end{bmatrix} \qquad (2\text{-}12)$$

$$Rot(y, E_S) = \begin{bmatrix} \cos(E_S) & 0 & \sin(E_S) \\ 0 & 1 & 0 \\ -\sin(E_S) & 0 & \cos(E_S) \end{bmatrix}$$

When aircraft rotated in the inertial reference, the included angles between LL frame and AC frame are roll, pitch, and yaw angles, with notation are **α**, **β**, and **γ** respectively, called aircraft Euler angles. The transformation sequence is in the Z-Y-X Euler angles form, and it is obtained by the gyroscope measurement. Therefore, the transformation from LL to AC frame is a rotation matrix

$$C_{LL}^{AC} = Rot(z, \gamma) Rot(y, \beta) Rot(x, \alpha) \tag{2-13}$$

where $Rot(x, \alpha)$, $Rot(y, \beta)$ and $Rot(z, \gamma)$ are

roll axis: $\quad Rot(x, \alpha) = \begin{bmatrix} 1 & 0 & 0 \\ 0 & \cos(\alpha) & -\sin(\alpha) \\ 0 & \sin(\alpha) & \cos(\alpha) \end{bmatrix}$

pitch axis: $\quad Rot(y, \beta) = \begin{bmatrix} \cos(\beta) & 0 & \sin(\beta) \\ 0 & 1 & 0 \\ -\sin(\beta) & 0 & \cos(\beta) \end{bmatrix}$ $\tag{2-14}$

yaw axis: $\quad Rot(z, \gamma) = \begin{bmatrix} \cos(\Upsilon) & -\sin(\Upsilon) & 0 \\ \sin(\gamma) & \cos(\Upsilon) & 0 \\ 0 & 0 & 1 \end{bmatrix}$

To get final antenna gimbal angle commands, we should transform the antenna LOS vector in S frame into AC frame using the direction cosine matrices. Combining equation (2-11) and (2-13) the antenna LOS unit vector in AC coordinate is

$$\overrightarrow{u_{LOS}^{AC}} = C_{LL}^{AC} \cdot C_s^{LL} \cdot \overrightarrow{u_{LOS}^{S}} \tag{2-15}$$

Since the Euler angles are in Cartesian coordinate space, but in our radar

gimbal mechanism is defined in sphere coordinates, we will transform from the Cartesian space to the sphere space or from the sphere space to the Cartesian space. And we assumed that the unit vector in radar antenna coordinates by following

$$\overrightarrow{u_{LOS}^{AC}} = \begin{bmatrix} u_x \\ u_y \\ u_z \end{bmatrix} \tag{2-16}$$

where $\overrightarrow{u_{LOS}^{AC}}$ is the servo command for three dimensions in Cartesian space. The servo errors should be zero when the antenna is aligned to the unit vector. In our radar gimbal mechanism, there are only two axes to stabilize the aircraft body rotation which has three rotation degrees of freedom. There, the final commands order to antenna gimbals can be written in arctangent form by

$$\text{Azimuth:} \qquad \theta_{AZ} = \tan^{-1}(\frac{-u_x}{u_y})$$

$$\tag{2-17}$$

$$\text{Elevation:} \qquad \theta_{EL} = \tan^{-1}(\frac{u_z}{\sqrt{u_x^2 + u_y^2}})$$

During antenna pointing a target on the ground, the position loops are closed to remove gyro drift and servo position biases accumulated during the scan bar. The gimbal angle commands are continually updated according to the above process when the position loops are closed.

Chapter 3 Antenna Stabilization System

Antenna stabilization is concerned with the relationship between antenna and aircraft. It is necessary to establish a complete system, includes sensors, actuators, mechanism, controller and the Human Machine Interface (HMI) to meet the stabilization requirement. The antenna stabilization system must direct the antenna LOS to ensure gapless earth coverage in different operation modes. With inertial measurement data consisting of the aircraft's position, velocity, and attitude, algorithm generates required gimbal angles and LOS inertial rate commands that ensure the radar's image will cover a designated earth-fixed region with minimum overlap. The hardware includes a combination of inertial measurement sensors, actuators and antenna gimbal mechanism. It attempts to keep the antenna gimbal mechanism pointing to a fixed direction while a map is being made. As some maps take tens of seconds to produce, the stabilization systems must be able to hold the antenna stable over this period.

3.1 Antenna Stabilization

Consider a radar installed on board an aircraft whose velocity is *v* and that has roll, pitch, or yaw motion. A conformal map of the ground configuration will be obtained by compensating for the platform movements and stabilizing the radar antenna relative to the platform. In the case of an electronically steered antenna, steering commands for both angle tracking and space stabilization must be provided. To continuously correct for changes in aircraft attitude, no matter how small, new commands must be computed and fed to the antenna at a very high rate.

The whole flowchart of airborne radar reconnaissance system is shown in Figure 3.1. It includes the antenna, stabilizer, Inertial Measurement Unit (IMU), data controlling and recording units. The position and attitude data of the antenna for each time instance are acquired with IMU and it consists of two parts: Global Position System (GPS) and gyroscope. GPS is that a network of 24 satellites continuously transmits high-frequency radio signals, containing time and distance data that can be picked up by any GPS receiver, allowing the user to pinpoint their position anywhere on Earth. It has 1 hertz update rate to correct the drifted error caused by Earth's itself rotation. From GPS, the WGS-84 coordinates is adopted. The gyroscope consists of three magnetometers, three accelerometers, and three rate gyroscope sensors to measure the attitude data of aircraft. With these data transmitting to host computer for real-time computations, the commands for antenna stabilization are generated.

The antenna is fitted with a stabilizer, followed by a servo-loop mechanism. The direction of the antenna beam is controlled by the servos, which drive the antenna gimbal structure in two axes, called azimuth and elevation. The azimuth servo rotates the whole structure about a vertical axis, thereby changing its heading relative to north. The elevation gimbal rides on the rotating azimuth carriage, and tilts the antenna boresight upward and downward relative to the horizontal plane. The servomechanism stabilizes the antenna pointing angle such that antenna LOS can be direct to designated earth-fixed locations. Due to the high-performance stabilizer, an acquired original image has no jitter and no blur. Therefore these images are suitable for real-time processing in emergency cases, where the burden for post-processing must be reduced.

3.2 Hardware Introduction

Presently the stabilizers for airborne reconnaissance system which foreign companies invented are usually two or four axes gimbal mechanism. Figure 3.2 shows three present airborne stabilizer products, which (a) and (b) are for EO sensor application, and (c) is for radar application. The stabilizer should stabilize the sensor or antenna LOS regardless of aircraft motion while a map is being made.

Likewise we design an antenna servomechanism. It is the most important elements of the antenna assembly and composed of three parts. The gimbal mechanism supports the antenna. The motor and associated drive provide the driving force. The gyroscope senses the antenna pointing angles and provides an input for feedback control. The stabilization loop ensures proper feedback control while antenna is pointing a designated direction.
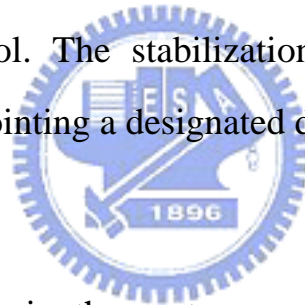
3.2.1 D.C. Servomotor

The motor we chose in the system as actuator is SmartMotor 2315D. Traditionally, an entire servomotor system includes: encoder, motion controller, driver, servomotor, and cables etc. The SmartMotor integrates these components in a single module, and it becomes an integrated servo system. It includes a very high quality, high performance brush-less D.C. servomotor which has a rotor with extremely powerful rare earth magnets and a stator (the outside, stationary part) that is a densely wound multi-slotted electro-magnet. There are seven I/O channels available on a SmartMotor 2315D. They can be assigned as either inputs, outputs, or 10 bit analog inputs individually. Besides, there is also an encoder which resolution is 2000 counts/revolution coupled to the motor shafts to provide feedback signals for the position feedback loops. The servomotor

works with a D.C. power supplied 24 volts and its communication are under the RS232 interface.

The major advantage for our selection is system volume reduction. With all components integrating in a single servomotor module, we can efficiently reduce system volume. The SmartMotor is shown in Figure 3.3.

3.2.2 Gyroscope

The gyroscope measures the changing attitudes of aircraft which are absolute roll, pitch, and yaw angles. The gyroscope we chose is MicroStrain 3DM-G. It is a self-contained sensor system that measures the three degrees of its orientation in space with respect to Earth. When we say Earth, we are referring to the coordinate system established by the cardinal axes of our planet Earth itself. We define a coordinate system that is "fixed" to the Earth with the Z-axis pointing down through the center of the Earth, the X-axis pointing North and the Y-axis pointing East. By 'fixed' we mean that this coordinate system is stationary and provides us with a reference to measure against. The Earth's Coordinate System is shown in Figure 3.4.

Likewise we define a local coordinate system that is fixed to the gyroscope. The MicroStrain 3DM-G is shown in Figure 3.5. The faceplate is imprinted with the gyroscope's coordinate system for reference during use. The measurements output by the gyroscope give the orientation of the gyroscope's local coordinate system with respect to the Earth's coordinate system. If we orient the gyroscope such that its Z-axis is pointing down through the center of the Earth, its X-axis is pointing north and its Y-axis is pointing east, we have aligned the gyroscope with Earth's coordinate system. At this orientation the gyroscope will be outputting zero pitch, zero roll and zero yaw angles. If we turn it from there, we

will start getting non-zero pitch, roll and yaw angles.

The 3DM-G incorporates:

- ◆ accelerometer sensor to measure Earth's gravity

- ◆ magnetometer sensors to measure magnetic fields

- ◆ rate gyroscope sensors to measure the rate of rotation about their sensitive axis

- ◆ a temperature sensor

- ◆ signal conditioning amplifiers to condition the raw output of the sensors

- ◆ a signal multiplexer to route the sensors' signals to the A/D converter

- ◆ a 12-bit A/D converter that converts the conditioned output of the sensors into the digital domain

- ◆ a microprocessor that carries out the processing algorithm

- ◆ non-volatile EEPROM to store calibration, filter and other parameters

- ◆ a data communications port

3.2.3 Two-axis Gimbal Mechanism

Referring to most stabilizer design, the antenna is fitted with a roll-stabilizing system followed by the servo-loop in azimuth carrying an elevation servomechanism. We use a two-axis gimbal mechanism equipped two D.C. servomotors to stabilize antenna. The gimbal in Figure 3.6 and Firgure3.7 are the prototype of antenna gimbal mechanism designed by Yong-Chieng Tong in our laboratory. It is designed for the purpose of high efficiency and least power loss in a small workspace. That is just suitable for airborne side–looking radar.

We define the gimbal rotation angles as follows:

◆ Azimuth angle (AZ): The angle between the projection of the antenna centerline onto the x-y plane of the S frame, often termed the azimuth component of the look angle.

◆ Elevation angle (EL): The angle between the antenna centerline and its projection onto the x-z plane of the S frame, often termed the elevation component of the look angle.

The azimuth range is ± 15 degrees and the elevation range is ± 40 degrees for our gimbal. The gimbal support assembly has been designed to specifically match the UAV structure, but that can be easily modified to fit other aircraft mounting configurations. It can be looked as an actively inertial stabilized platform to stabilize antenna's inertial position. Its SolidWork sketch and actual picture are shown in Figure 3.8 and Figure 3.9.
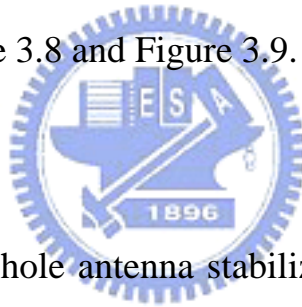
3.3 System Architecture

The architecture of whole antenna stabilization system is shown in Figure 3.10. When the heading angle H_m and elevation angle E_s are given, a target unit vector from antenna to target is decided in LL frame. Gyroscope measures the changing attitudes of aircraft which are absolute roll, pitch, and yaw angles, and transmits them to host computer. Stabilization program of host computer receives the gyroscope data, and calculate the final commands to antenna gimbals through a series of coordinate transformations. By host computer real-time sending commands to servomotors, gimbal mechanism can continuously point the antenna LOS at the desired direction (azimuth and elevation) in the space regardless of aircraft motion.

Two servomotors are connected to a single RS-232 port as Figure 3.10 shown. The method is called "daisy chain", and it makes the communication

between host computer and servomotors just need one RS-232 port. For independent motion, however, each motor must be programmed with a unique address. The consecutive nature of the RS-232 daisy chain creates the opportunity for the chain to be independently addressed entirely from the host, rather than by having a uniquely addressed program in each motor. Setting up a link this way can add simplicity because the program in each motor can be exactly the same.

Considering the antenna gimbal is mounted on the aircraft, all components should be limited in a restricted space. In the cause of cables assembly convenience, an integrating assembly circuit is designed to integrate all necessary circuits. The integrating assembly circuit diagram is shown in Figure 3.11. It integrates power, all communication, and photointerrupter circuits in a single electrical board. In order to prevent motor rotate over its working space, a pair of photointerrupters is used to limit the motor's position for each axis motion. When motor rotates over its working space, the photointerrupter will be obstructed and induce a voltage drop from 5V to 0V to the input port of servomotor. After receiving the low signal, the servomotor will stop emergently. The photointerrupters is utilized as the hardware limit of antenna gimbal mechanism, thus we can efficiently prevent excessive motion causes mechanism damages. The photointerrupter circuit is shown in Figure 3.12.

In order to implement high performance antenna stabilization system, PC–based controller is the best choice for high speed calculation, real-time operation, easy programming, expansion ability and good feasibility. The design of HMI becomes simple and extensible by Microsoft Victual C++. The antenna stabilization HMI is shown in Figure 3.13. It consists four major parts. Part one shows the aircraft inertial attitudes and body axis angular velocities. Part two

shows the encoder values of servomotors, and host computer can also directly command servomotors in the program. Part three is used to input the heading angle H_m and elevation angle E_s, and generates the target unit vector in LL frame. Part four gives several functions for antenna stabilization, which includes antenna gimbal homing, reset the inertial frame, motor servo off and emergency stop etc.

Finally, an iron board is used to simulate radar disk, and a red-light laser pointer is installed in the perpendicular board direction to simulate antenna LOS for experience convenience. The antenna gimbal LOS can be obviously determined if it is in the desired direction according to the pointer beam. The actual picture of antenna stabilization system is shown in Figure 3.14.

Chapter 4 System Performance Analysis

For antenna tracking of a target in angle employs a servo system that utilizes the angle-error signals to maintain the pointing of the antenna in the direction of the target. Figure 4.1 shows the block diagram for both axes of the angle-tracking servos, which position the antenna in azimuth and elevation. Encoders are coupled to the motor shafts, to provide feedback signals for the position feedback loops closed around the antenna drives. The inertial position loops control the pointing position of the antenna with respect to a LL frame. With the PID controller, steady-state error can be reduced to zero and transient state response can be appropriate adjustment.
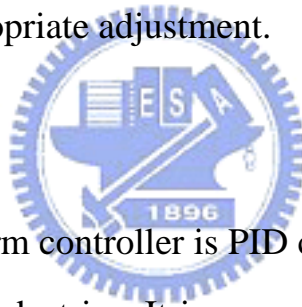
4.1 PID Controller

The classical three-term controller is PID controller, and it is widely used in the process and robotics industries. It is composed of Proportional Control (P), Integral Control (I), and Derivative Control (D). The control law is described by

$$u(t) = K_p e(t) + K_I \int_0^t e(\tau) d\tau + K_D \frac{de(t)}{dt} \qquad (4\text{-}1)$$

where $e(t)$ is error signal; $u(t)$ is reference input signal; K_p is proportional gain; K_I is integral gain; K_D is derivative gain.

The proportional feedback control (P) can reduce error responses to disturbances but that it still allows a nonzero steady-state error to constant inputs. When the controller includes a term proportional to the integral of the error (I), then the steady-state error can be eliminated and the disturbance can be canceled, although typically at the cost of deterioration in the dynamic response. Addition

of a term proportional to the derivative of the error (D) can often improve the dynamic response by reducing the oscillation while maintaining zero steady-state error.

Equivalently, the control law is also represented as

$$K_p \left(e(t) + \frac{1}{T_I} \int_0^t e(\tau)d\tau + T_D \frac{de(t)}{dt} \right) \tag{4-2}$$

Then the transfer function of PID controller is described by

$$\frac{U(s)}{E(s)} = K_p \left(1 + \frac{1}{T_I s} + T_D s \right) \tag{4-3}$$

where the "reset rate" in seconds, T_I, and the "derivative rate", T_D also in seconds can be given physical meaning to the operator who must select values for them to tune the controller.[10] The block diagram is shown in Figure 4.2.

4.2 Ziegler-Nichols Tuning of PID Regulators

Ziegler and Nichols devised an approach for tuning the PID controller parameters in 1942, which provided acceptable closed-loop response for many systems. In the criteria for adjusting the parameters are based on evaluating the amplitude and frequency of the oscillations of the system at the limit of stability rather than on taking a step response.

To use the method, the proportional gain is increased until the system becomes marginally stable and continuous oscillations just begin with amplitude limited by the saturation of the actuator. The corresponding gain is defined as K_u (called the ultimate gain) and the period of oscillation is P_u (called the ultimate period). P_u should be measured when the amplitude of oscillation is as small as possible. Then the tuning parameters are selected as shown in Table 4.1.[10]

We used the method to develop a PID controller that met steady-state and

transient specifications for both tracking input references and rejecting disturbances. After tuning, the step response of AZ and EL axis motor are shown in Figure 4.2 where we gave a position command of 100 steps for each motor. Blue line is the position response, and red line is the position error response. The response graph displayed the steady state error was eliminated to zero and its overshoot was reduced as possible. However, AZ axis motor has still larger overshoot and oscillatory behaviors than EL axis motor because of its larger moment of inertia.

4.3 Experiment Result

After PID parameters configuration, we do an experiment to analyze the system performance under different frequency disturbances. The disturbances are defined by aircraft Euler angles. Without actual aircraft navigation data, the aircraft Euler angles are taken in the form of sine function to simulate aircraft motion in the air. The disturbances are given by

$$\text{roll axis} \qquad \alpha(t) = A_\alpha \cdot \sin(\omega \times 2\pi t) \text{ (rad/sec)}$$

$$\text{pitch axis} \qquad \beta(t) = A_\beta \cdot \sin(\omega \times 2\pi t) \text{ (rad/sec)} \qquad (4\text{-}4)$$

$$\text{yaw axis} \qquad \gamma(t) = A_\gamma \cdot \sin(\omega \times 2\pi t) \text{ (rad/sec)}$$

where $\omega = 5$ Hertz , $A_\alpha = 10^o$, $A_\beta = 7.5^o$, and $A_\gamma = 5^o$. The simulated Euler angles of aircraft body are illustrated in Figure 4.3.

The three-axis Euler angles coupled together generate gimbal angle command for each servomotor. Figure 4.4 and 4.5 shows the input and output responses of AZ and EL axis motors under the disturbances, and the system sampling time is 40 msec. The servo system introduces a time delay in the tracking that results in a tracking error shown in figures. The lag error will

depend on the system bandwidth the ability of the servo system to accommodate to changes in position, velocity, or acceleration. Comparison between Figure 4.4 and Figure 4.5, the AZ axis motor response has larger overshoot and oscillatory behaviors and longer time delay than EL axis because of its larger moment of inertia.

The antenna drive servos operate in terms of the azimuth-elevation gimbal axes of the antenna, but the antenna stabilizer computes the tracking error in terms of the comparison between antenna actual LOS and desired target vector in the inertial coordinate. To get actual LOS variation under aircraft motion in the inertial coordinate, we transformed the antenna LOS represented in S frame to EF frame with two output gimbal angles and three aircraft Euler angles by

$$U_{LOS}^{ef} = Rot(z,\gamma)Rot(y,\beta)Rot(x,\alpha)Rot(z,AZ)Rot(x,EL) \cdot U_{LOS}^{S} \qquad (4\text{-}5)$$

where $U_{LOS}^{S} = [0,1,0]^{T}$. The Actual LOS and desired LOS in inertial coordinate are shown in Figure 4.6.

The tracking error is defined by

$$E_{t} = \sqrt{\left[(L_{t})_{x} - (L_{o})_{x}\right]^{2} + \left[(L_{t})_{y} - (L_{o})_{y}\right]^{2} + \left[(L_{t})_{z} - (L_{o})_{z}\right]^{2}} \text{ (rad)} \qquad (4\text{-}6)$$

and the average of tracking error is

$$avg(E_{t}) = \frac{1}{n}\sum_{k=1}^{n}\sqrt{\left[(L_{t})_{x_{k}} - (L_{o})_{x_{k}}\right]^{2} + \left[(L_{t})_{y_{k}} - (L_{o})_{y_{k}}\right]^{2} + \left[(L_{t})_{z_{k}} - (L_{o})_{z_{k}}\right]^{2}} \text{ (rad)} \quad (4\text{-}7)$$

By the equation the average of tracking error is 0.222 (rad), and the function plot of tracking error is shown in Figure 4.7.

Likewise the system is simulated under actual disturbances by another experiment. The gyroscope is rotated by the random hand motion, and the results of antenna gimbal responses are shown in Figure 4.8 - Figure 4.13. The average of tracking error is 0.1526.

The steady state error can be efficiently reduced by PID control, but overshoot would be raised. The tracking error depends on amplitude and frequency of aircraft motion.

Chapter 5 Conclusion

The antenna stabilization system has been implemented and it provides the ability of continuously pointing the antenna LOS at the desired inertial position. The stabilizer is an azimuth carrying an elevation antenna gimbal servomechanism. For antenna tracking of a target in angle employs the servo system that utilizes the angle-error signals to maintain the pointing of the antenna in the direction of the target regardless of aircraft motion.

In the thesis, algorithm used for LOS control generates antenna gimbal commands. The antenna motion control is a closed feedback control. With the gimbal commands input to each axis motor, the encoder feed the output signals of motor back to the antenna motion controller and controller will do the PID control. To get better response, Ziegler-Nichols tuning method is taken as the reference of tuning PID parameters. The LOS tracking error is derived from encoders to analyze the system performance in the experiment.

HMI with several operation modes is also developed. The design of HMI becomes simple and extensible by Microsoft Victual C++. By integrating the inertial navigation, inertial measurement and recommending antenna gimbals tie in with the motion cleverly to operate the motion compensation, the stabilization automatically to avoid miss-pointing of the target. The antenna is said to be locked onto the target if the target return is continuously that accepts the commands from the controller and interfaces with the hardware. When the antenna gimbal shelf which simulated aircraft is rotated, the gimbal mechanism will rotate in an opposite direction to compensate.

In future, we can adopt different control methods more than PID to increase

the system performance further. The antenna stabilization system can be putted on the Steward platform with six degrees of freedom. Steward platform motion will affect the orientation of the antenna gimbal to simulate the real state of airborne radar system working on the aircraft.

Reference

[1] Byron Edde, <u>Radar Principle, Technology, Applications</u>, Prentice-Hall International 2nd Editions, 1993

[2] Philippe Lacomme, Jean-Philippe Hardange, Jean-Claude Marchais, Eric Normant, <u>Air and Spaceborne Radar Systems : An Introduction</u>, IEE, Norwich/New York, 2001

[3] George W. Stimson, <u>Introduction to Airborne Radar</u>, Second Edition, Scitech, New Jersey, 1998

[4] Dennis J. Kozakoff, <u>Analysis of Radome-enclosed Antennas</u>, Artech House, Boston/London, 1997

[5] Bogler, Philip L., <u>Radar Principles with Applications to Tracking Systems</u>, John Wiley & Sons, New York, 1989

[6] Daniel Levine, <u>Radargrammetry</u>, Mcgraw-Hill, New York/Toronto/London, 1960

[7] George Biernson, <u>Optimal Radar Tracking Systems</u>, John Wiley & Sons, New York/Hhichester /Brisbane/Toronto/Singapore, 1990

[8] Richard P. Paul, <u>Robot Manipulators: Mathematics, Programming, and Control</u>, MIY Press, 1981

[9] John J. Craig, <u>Introduction to Robotics Mechanics & Control</u>, Addison-Wesley Publishing Company, 1988

[10] Franklin G.F., Powell J.D., Abbas E.N., <u>Feedback Control of Dynamic Systems</u>, Fourth Edition, Prentice-Hall, 2002

[11] 楊憲束，<u>自動飛行控制原理與實務</u>，台北市，全華，民國 91 年

[12] Held K.J., Robinson B.H., "TIER II Plus airborne EO sensor LOS control

and image geolocation", IEEE Aerospace Conference Proceedings, Vol.2, pp.377-405, 1-8 Feb. 1997

[13] Tsuno, k., Grun, A., Zhang, L., Murai, S. , Shibasaki, R., "Starimager – a new airborne three-line scanner for large scale applications", Proceedings of ISPRS congress 2004, Istanbul, July 2004, digitally available on CD, 6 pages

[14] 何建興,「多目標追蹤雷達控制器」,國立交通大學,碩士論文,民國 90 年

[15] 楊嘉豐,「機載合成孔徑雷達訊號之運動補償」,國立交通大學,碩士論文,民國 93 年

[16] 王唯任,「液壓雷達穩定平台之設計、分析與控制」,國立清華大學,碩士論文,民國 90 年

[17] 黃淑鑌,「空用攝影偵照設備之減震定位平台」,國立清華大學,碩士論文,民國 90 年

Figures

Figure 2.1 Antenna LOS

(a) Without stabilizer   (b) With stabilizer
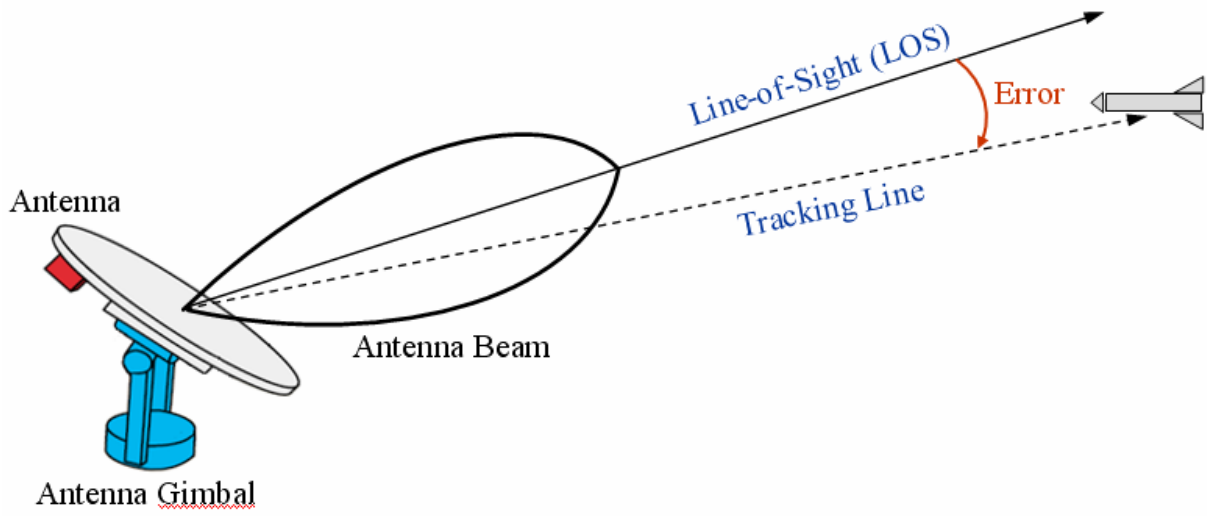
Figure 2.2 The stabilizer's effect on image quality
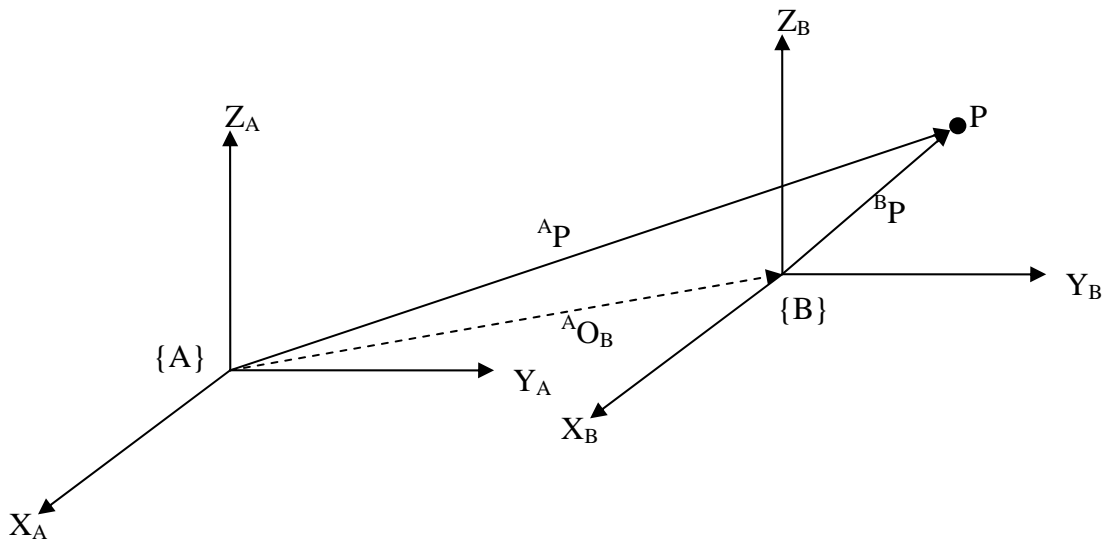
Figure 2.3 Translational mapping
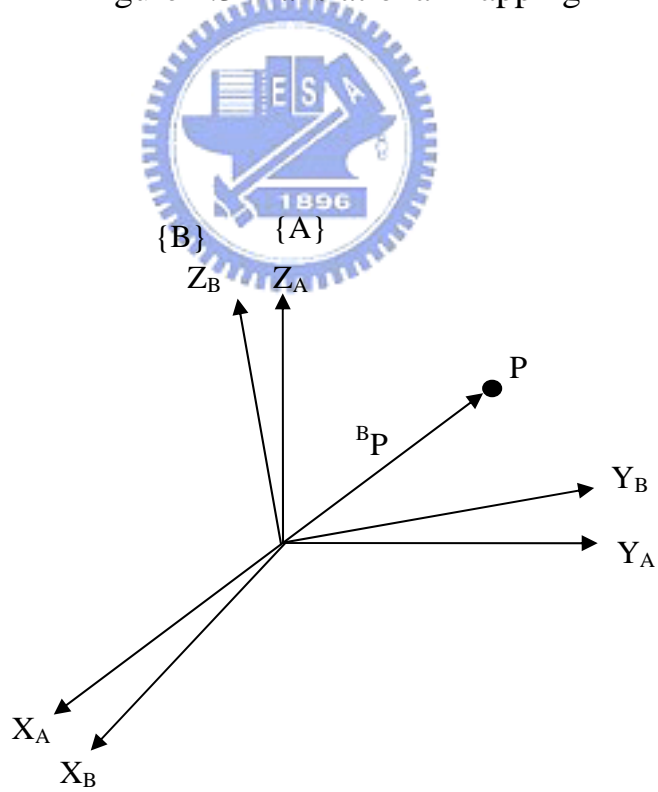
Figure 2.4 Rotational mapping
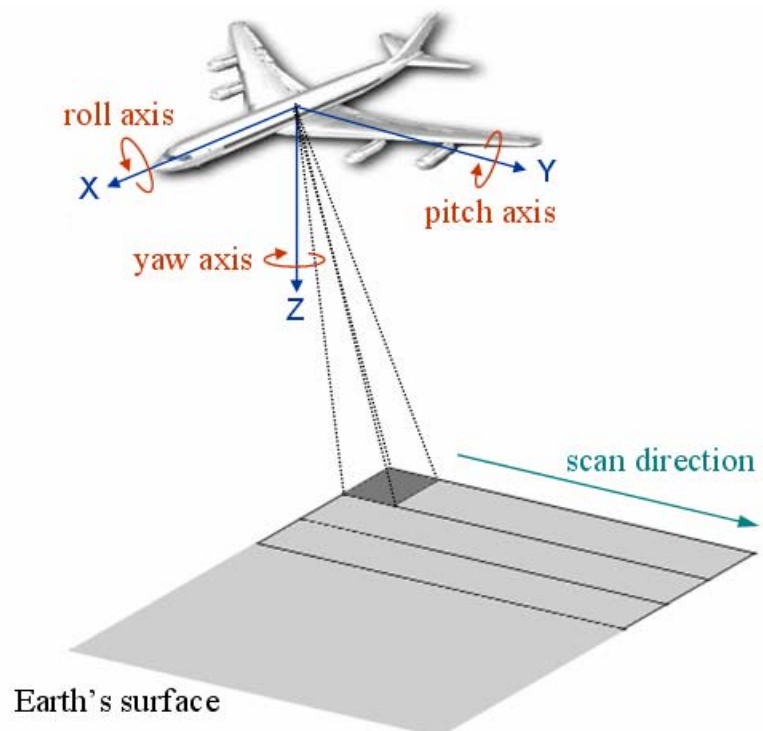
Figure 2.5 Wide Area Search mode
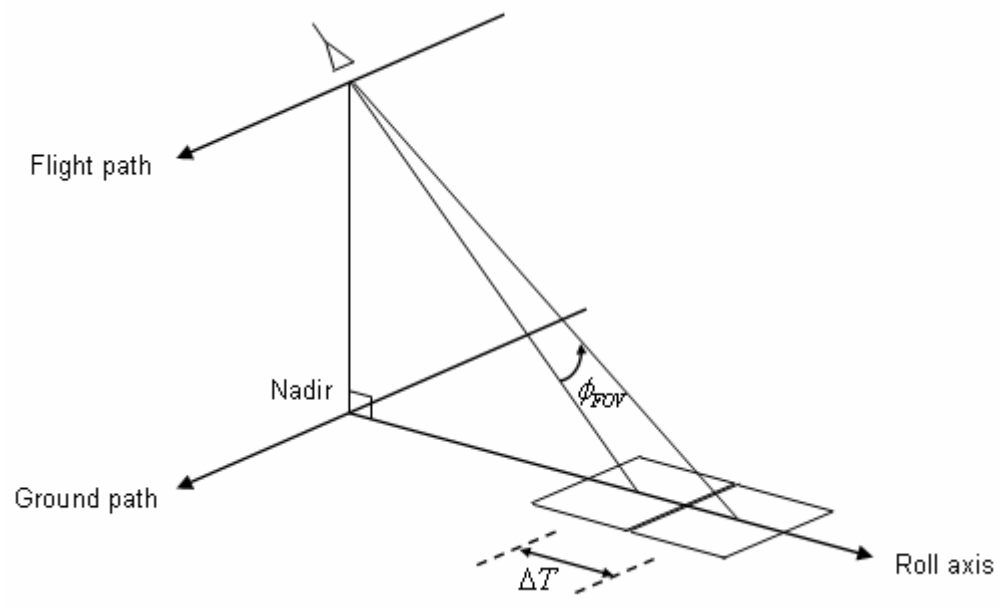
Figure 2.6 Geometry of Wide Area Search mode
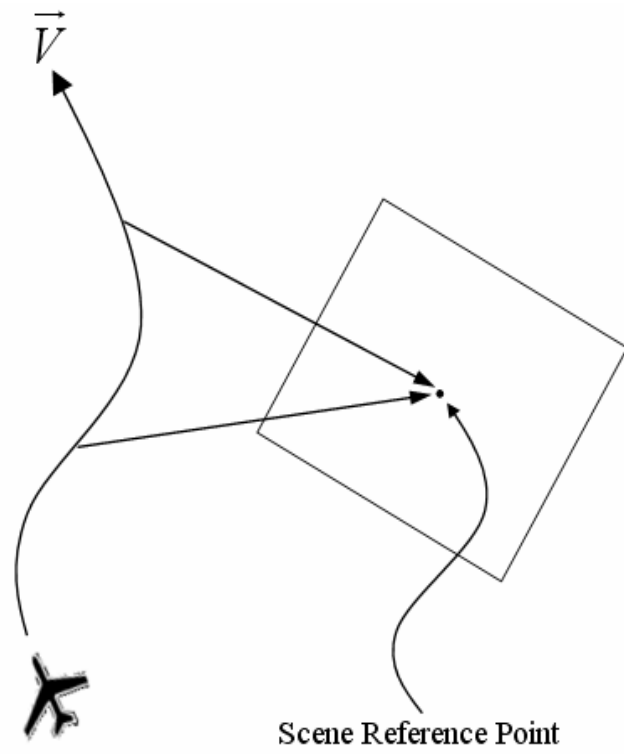
Figure 2.7 Spotlight mode
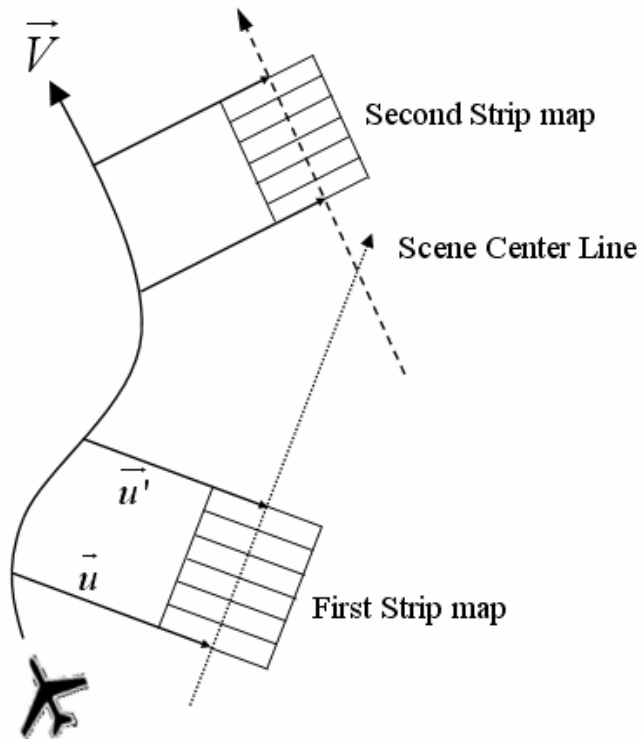
Figure 2.8 Stripmap mode
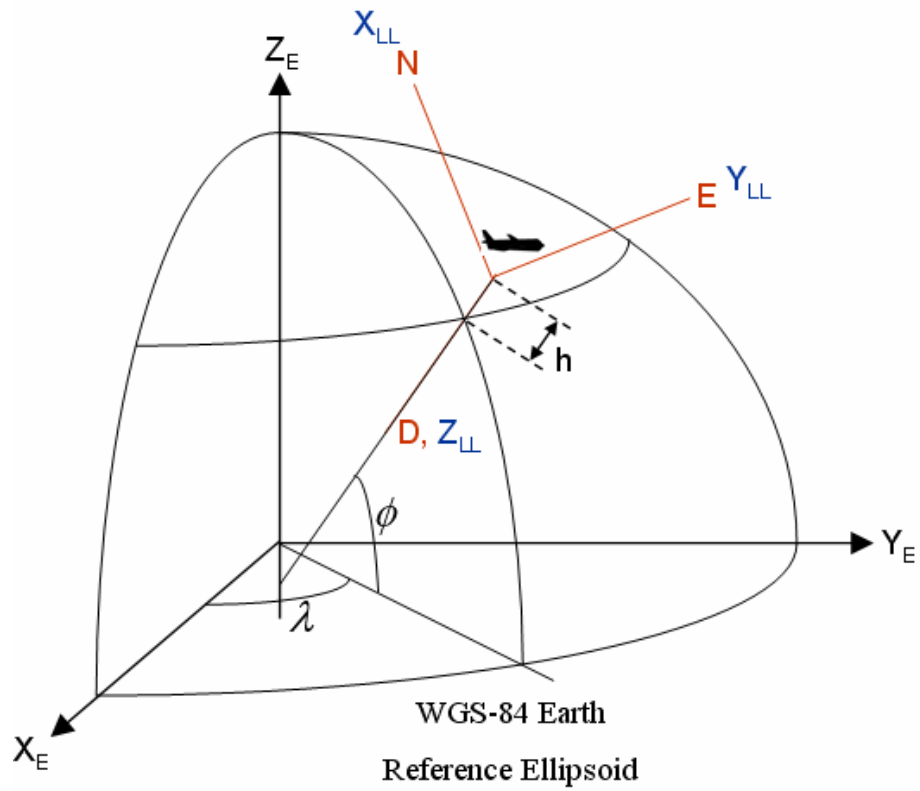
Figure 2.9 Coordinate frames for command generation
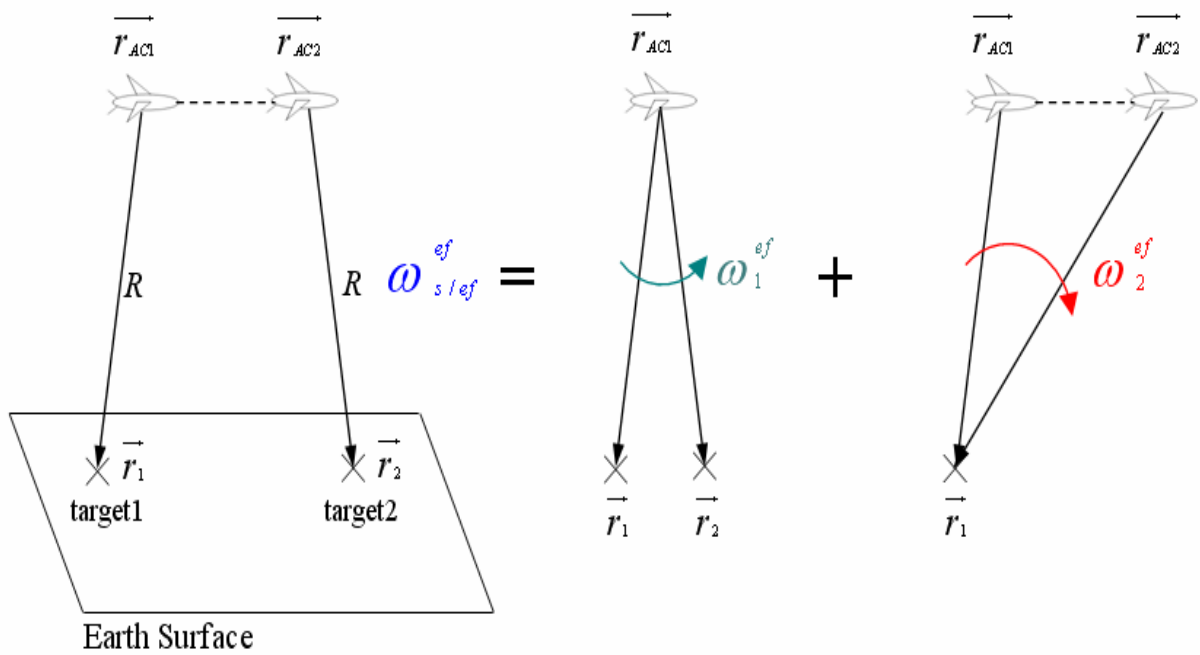
Figure 2.10 Inertial rate generator transfer partitioning mechanism
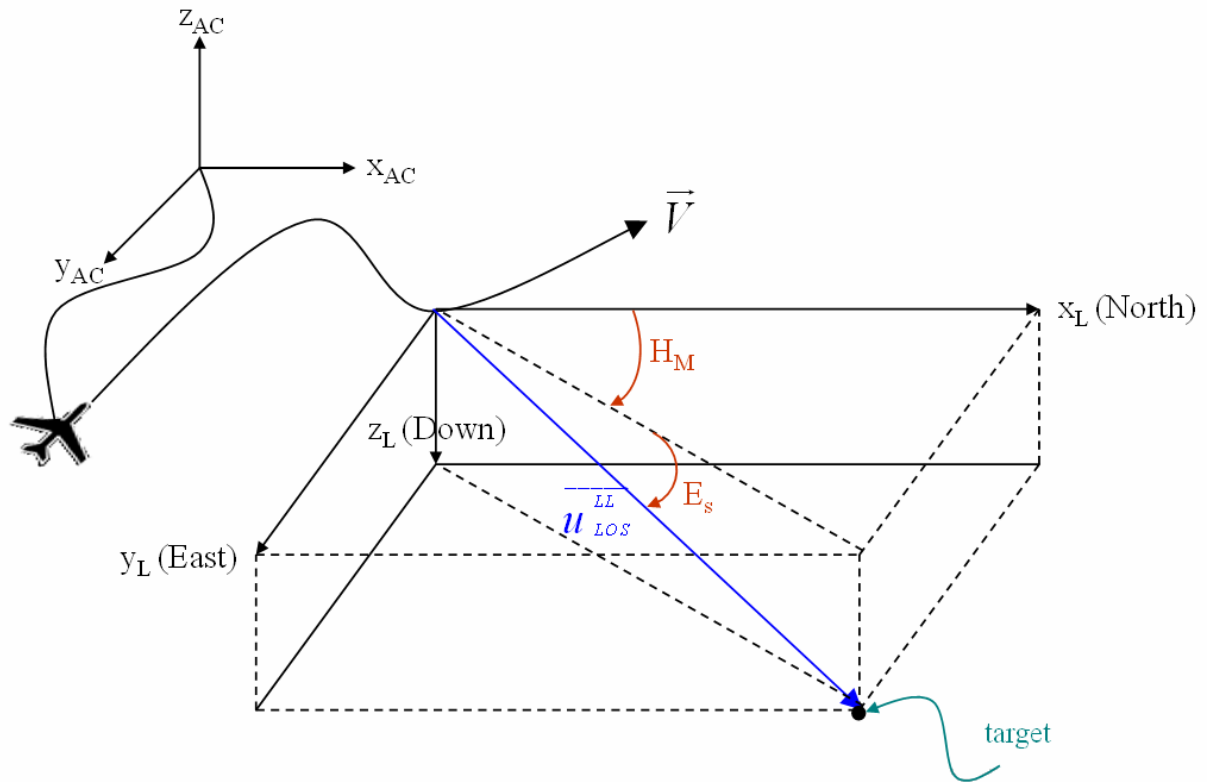
Figure 2.11 Geometry between antenna and target
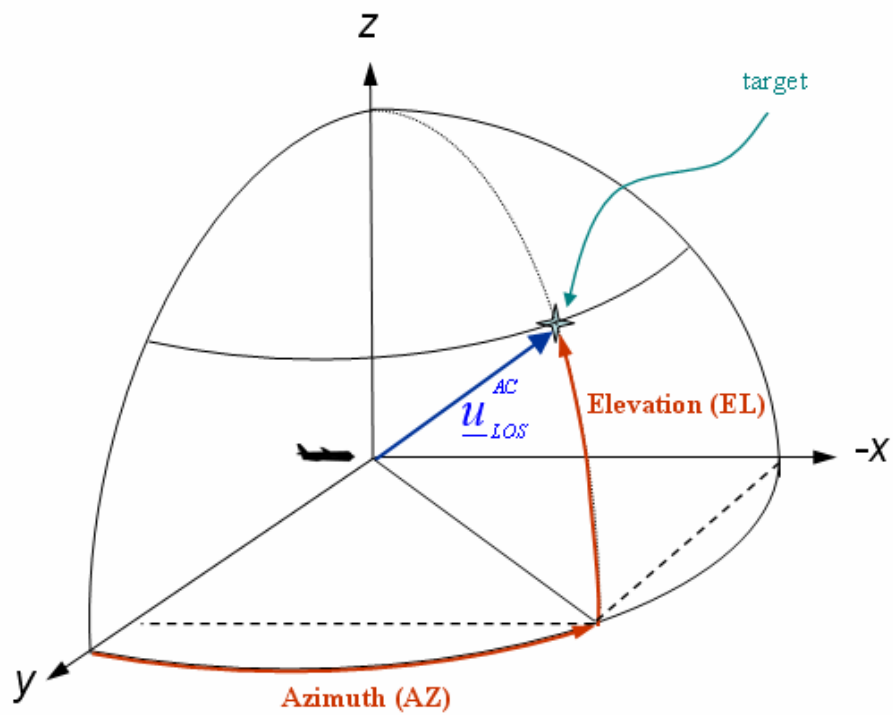
Figure 2.12 Antenna LOS in AC frame
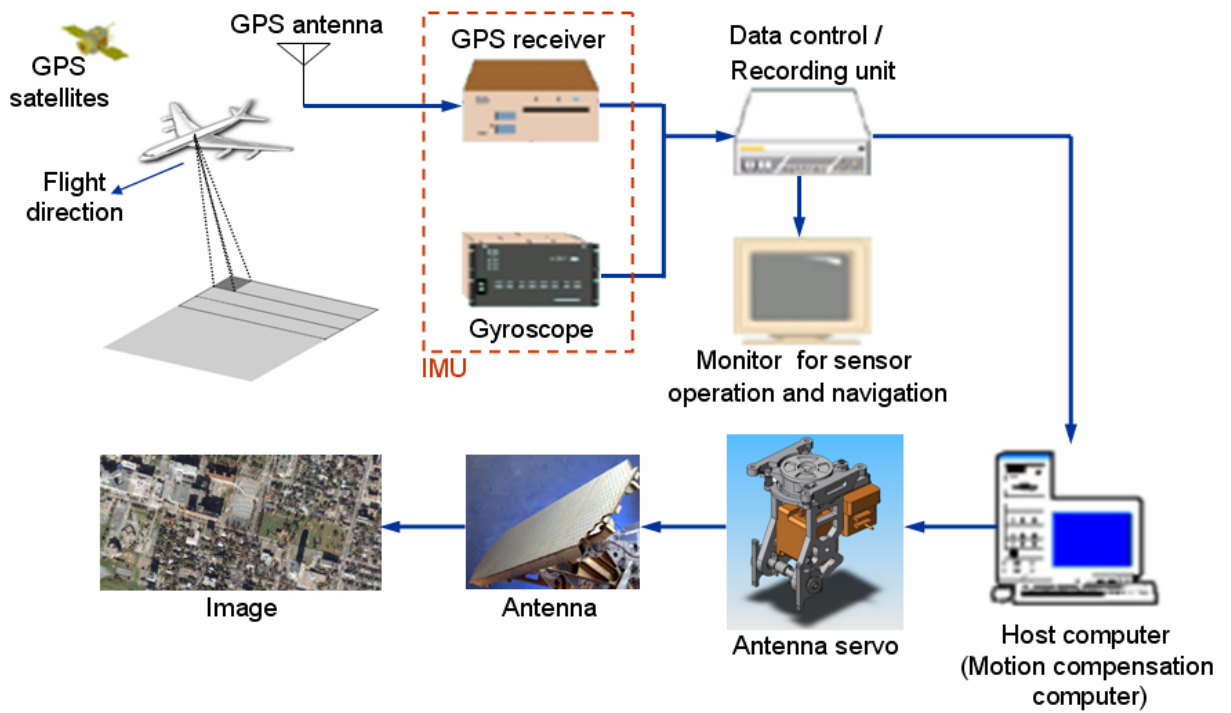
Figure 3.1 The flowchart of airborne radar reconnaissance system

(a) IAI
- MOSP

(b) Optical Alchemy
- KJ-600
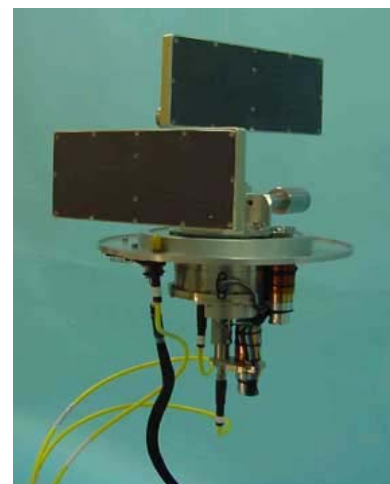
(c) Controp
- HRN-2

Figure 3.2 Present airborne stabilizer products

Figure 3.3 The SmartMotor 2315D
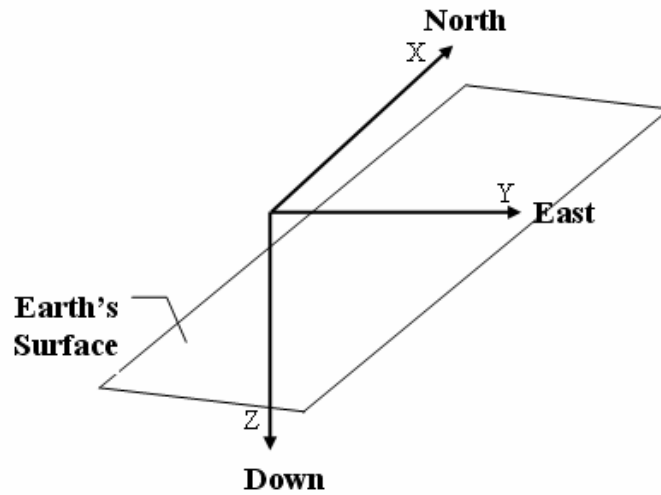
Figure 3.4 Earth's coordinate system

Figure 3.5 The gyroscope 3DM-G and its local coordinate
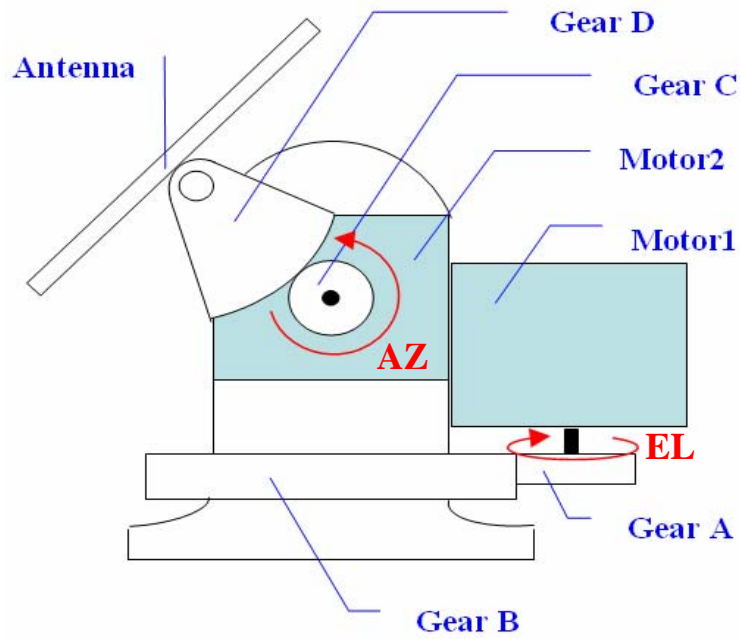
Figure 3.6 End view of gimbal mechanism
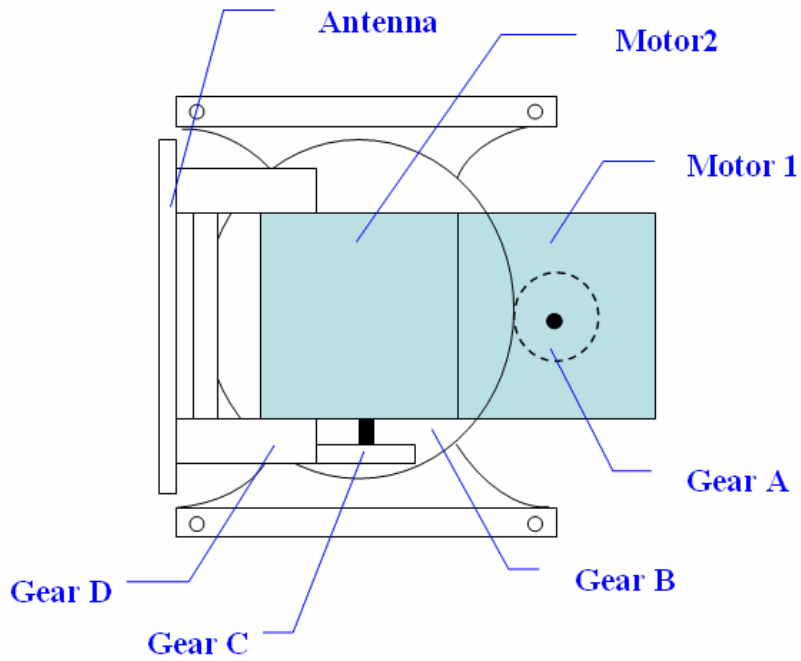
Figure 3.7 Front view of gimbal mechanism
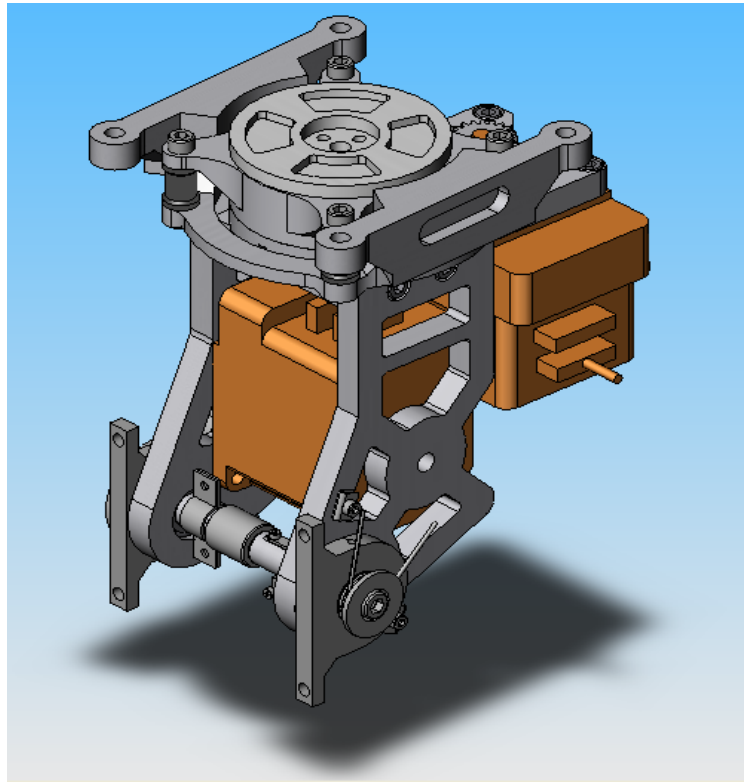
Figure 3.8 SolidWork sketch of gimbal mechanism

Figure 3.9 Actual picture of gimbal mechanism
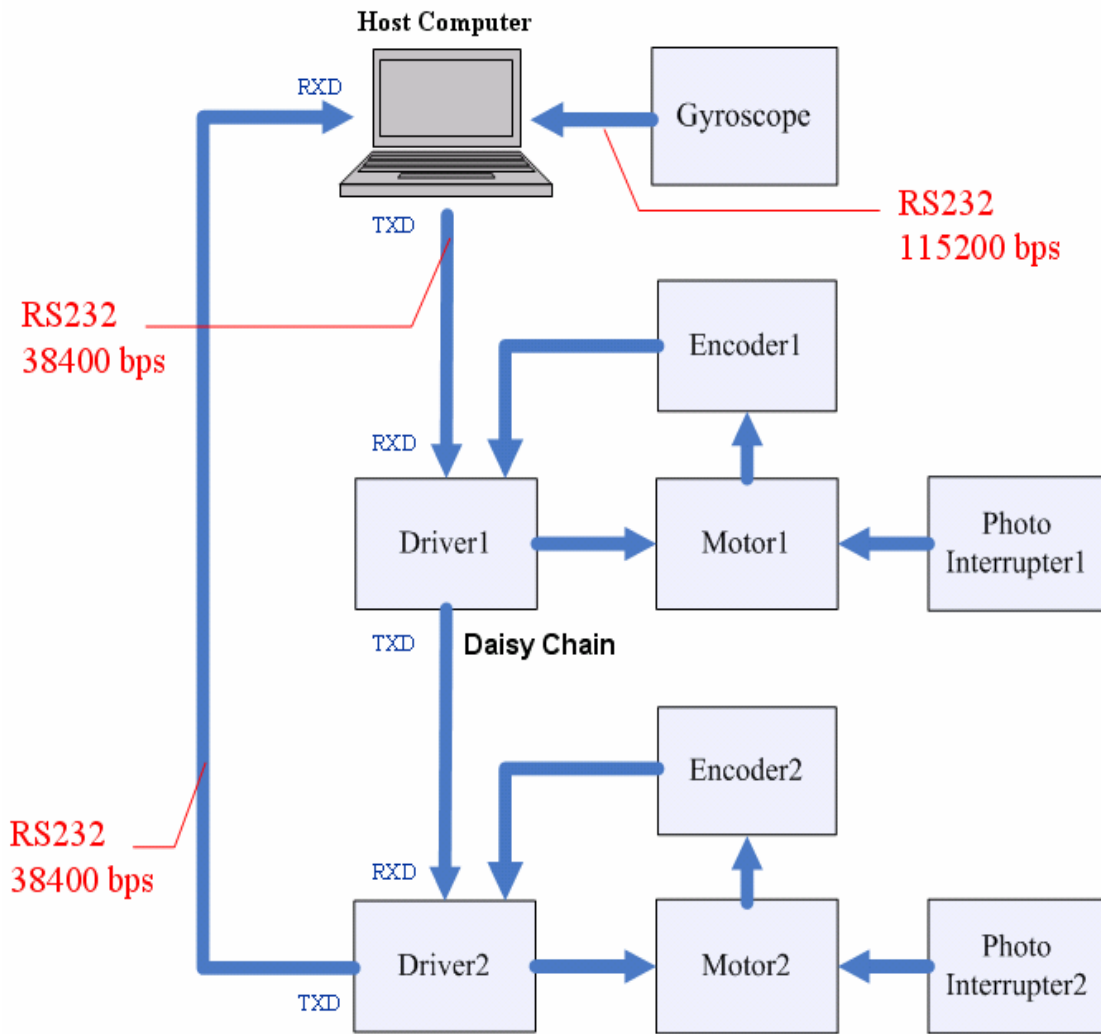
Figure 3.10 System architecture
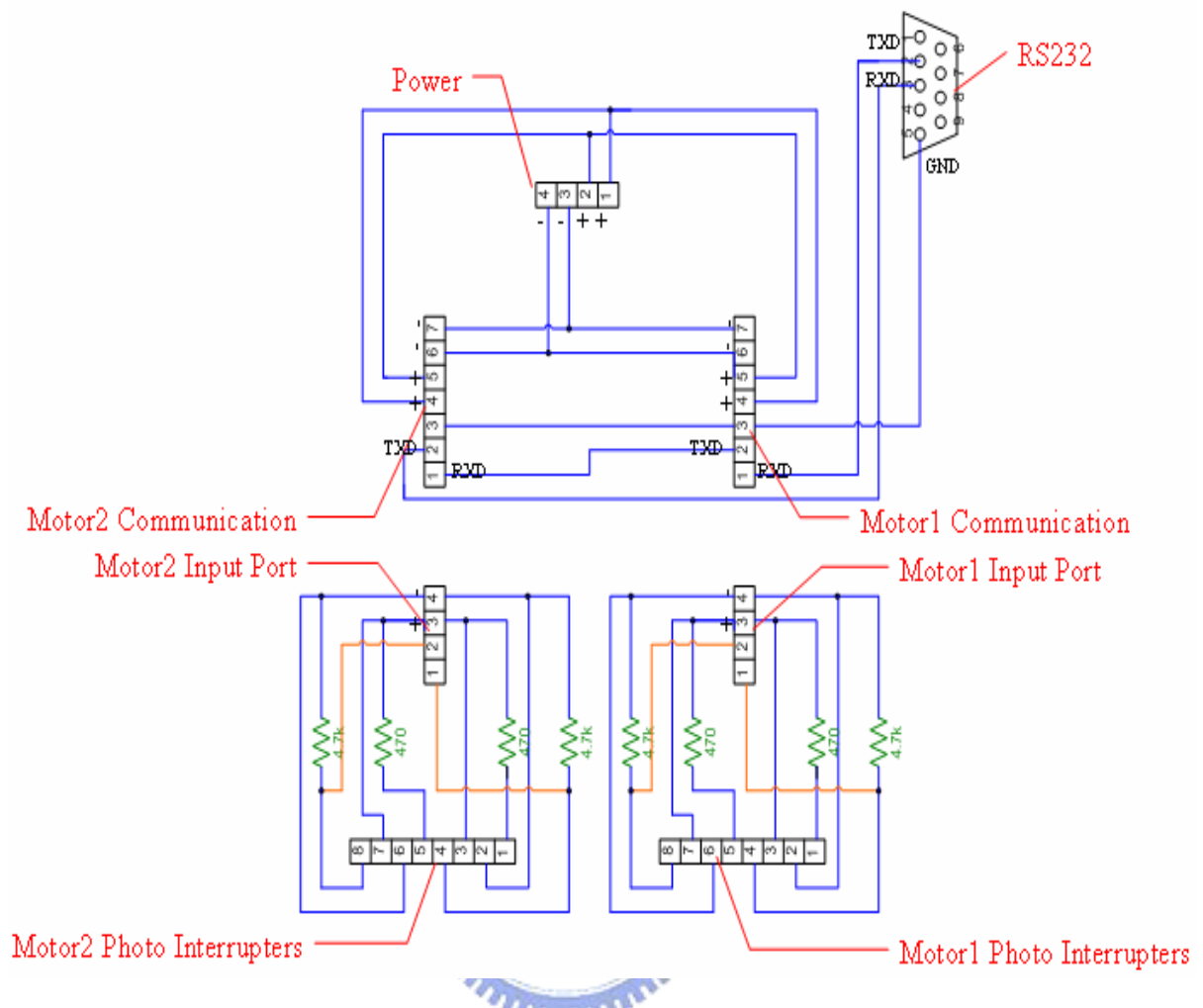
Figure 3.11 The integrating assembly circuit diagram
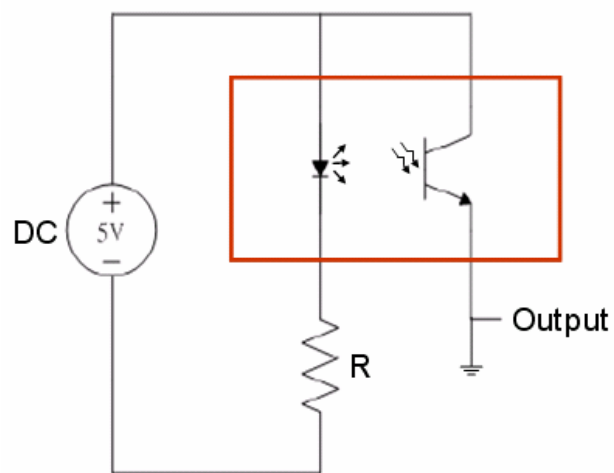
Figure 3.12 Photointerrupter circuit diagram
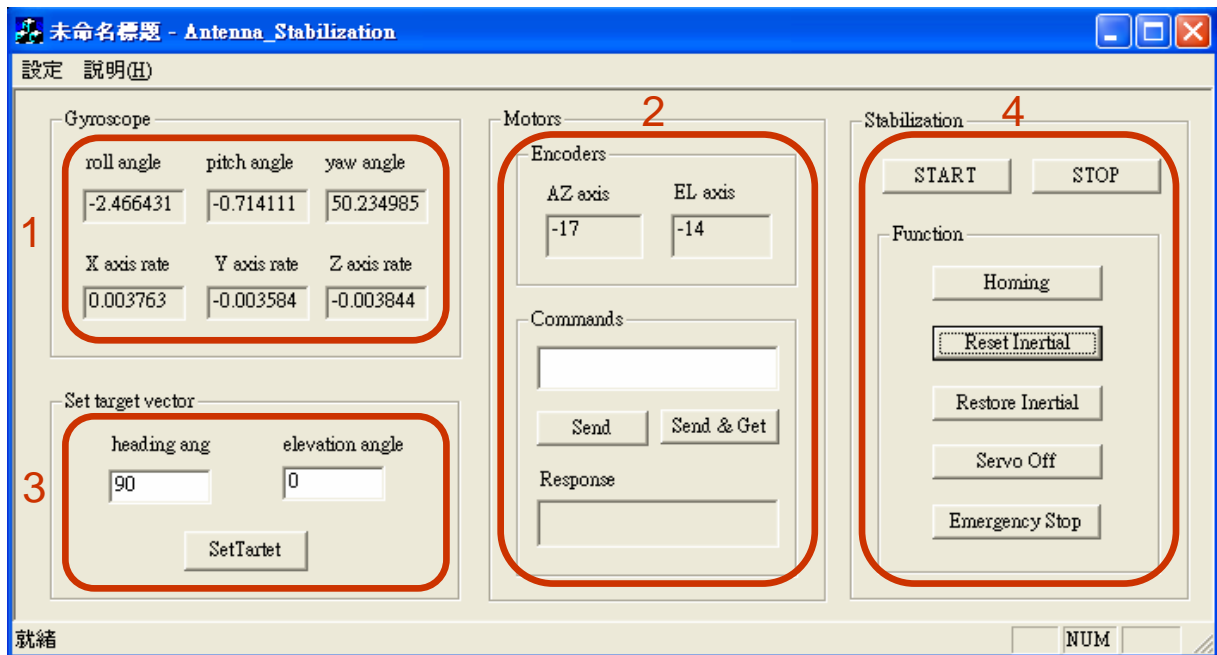
Figure 3.13 The Antenna stabilization HMI
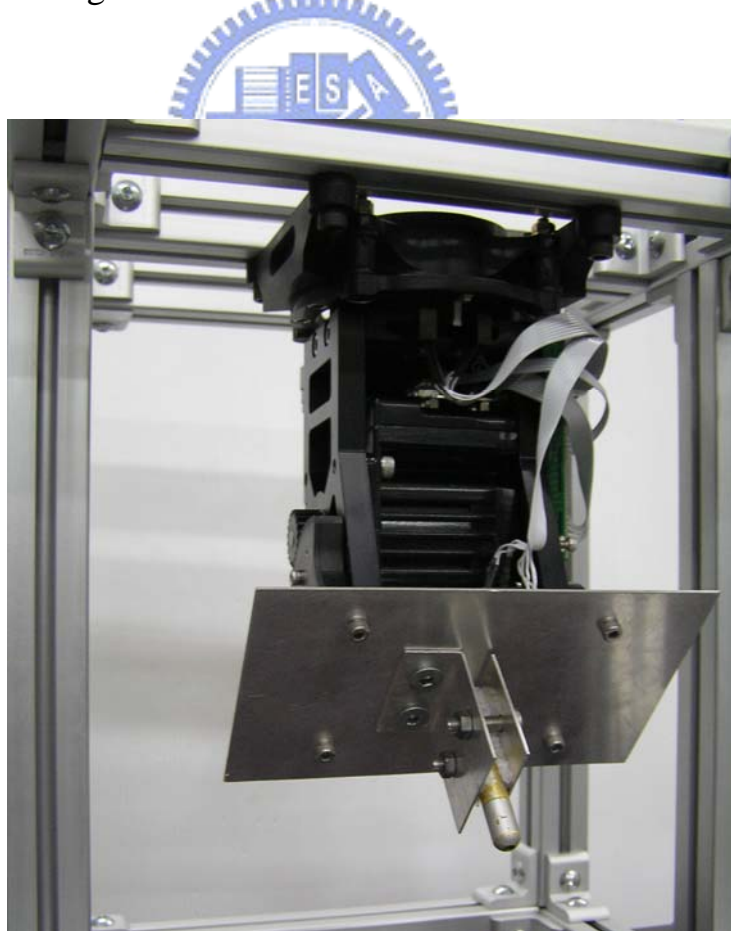
Figure 3.14 Actual picture of antenna stabilization system
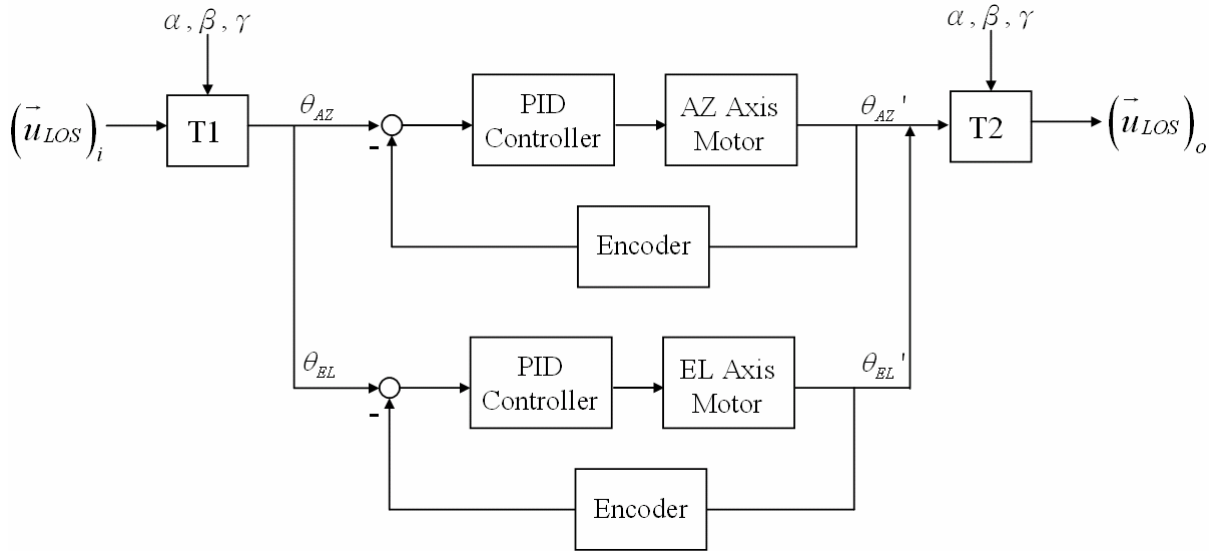
Figure 4.1 System block diagram
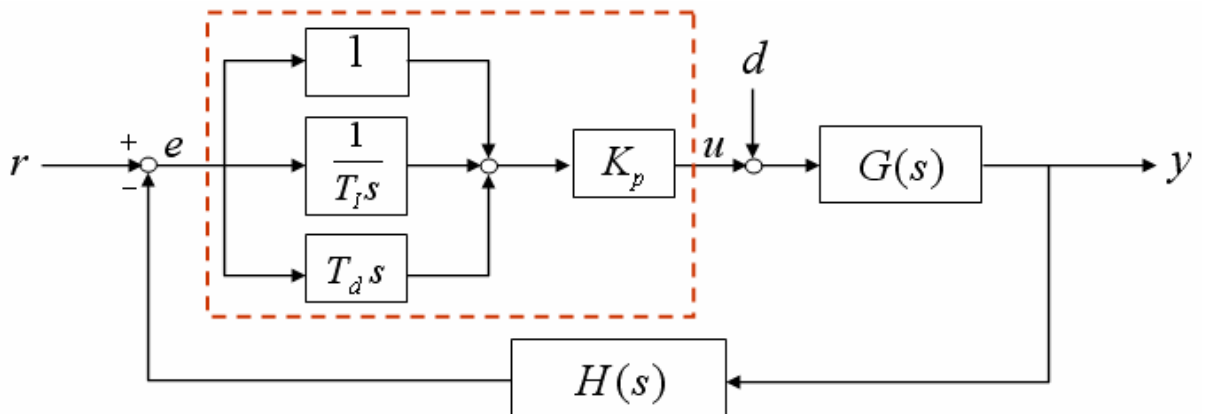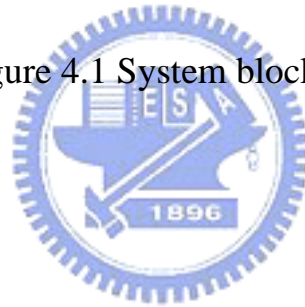
Figure 4.2 PID controller block diagram
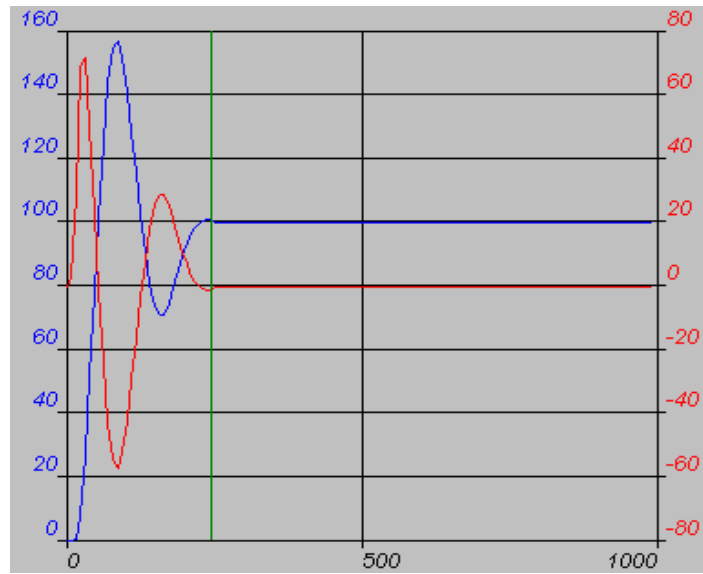
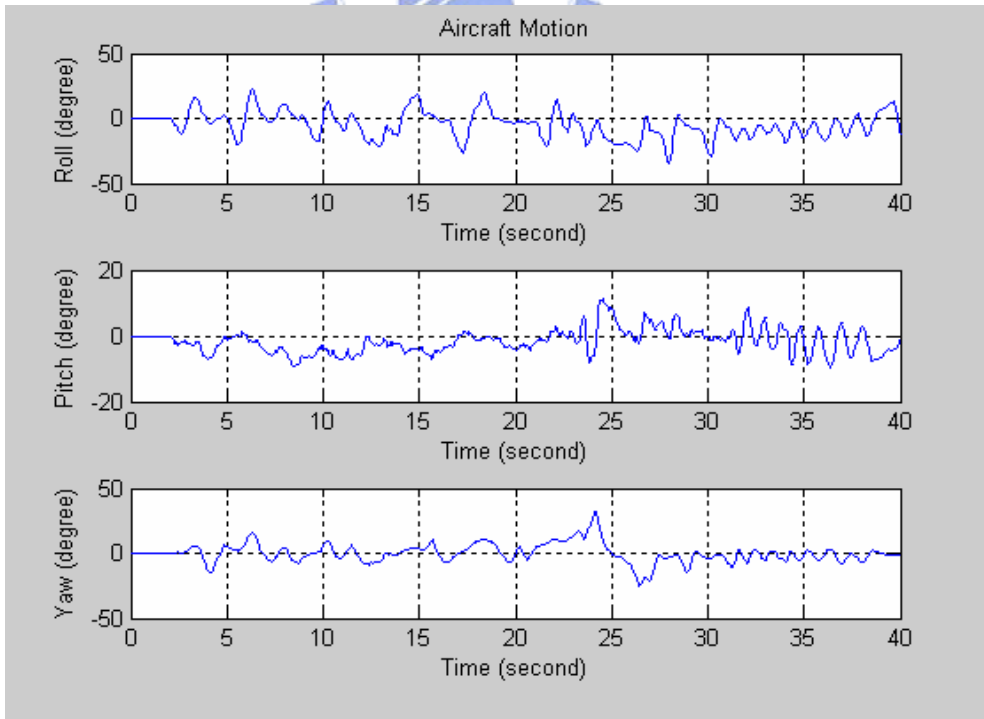(a) AZ axis motor
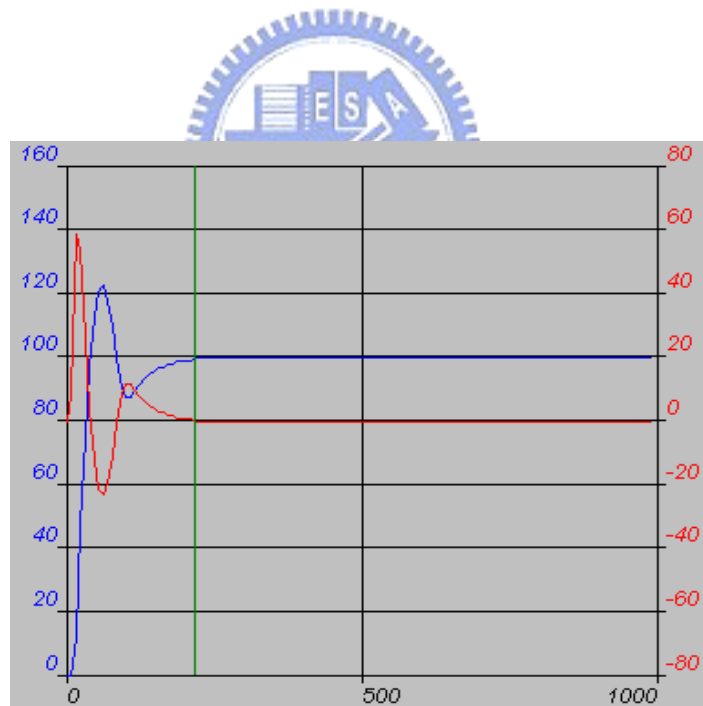
(b) EL axis motor

Figure 4.3 Step response of each motor
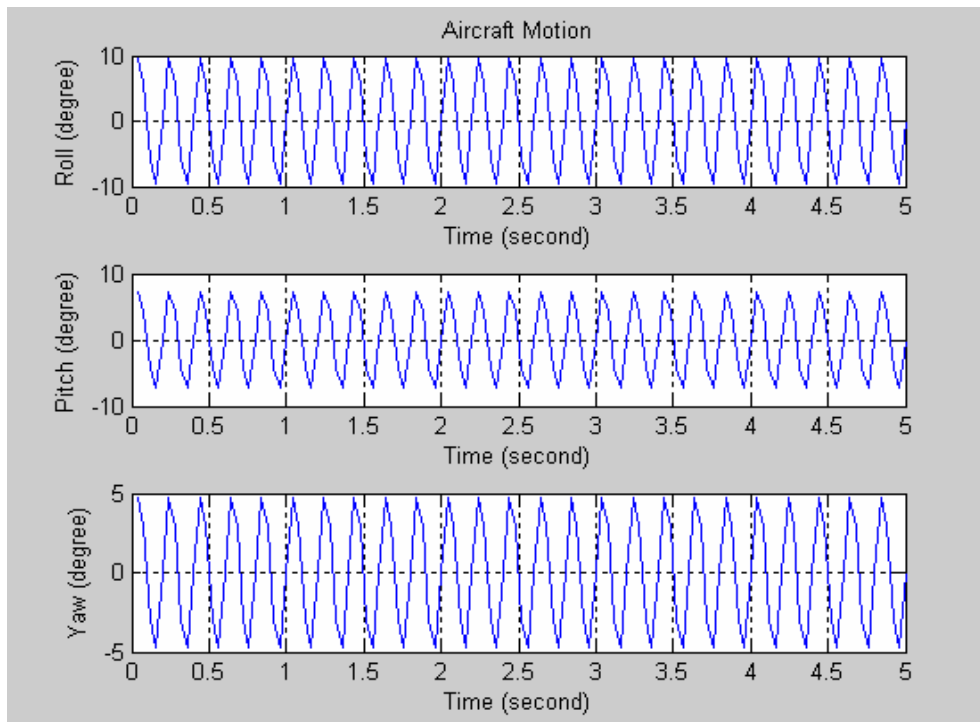
Figure 4.4 Euler angles of aircraft motion (5 Hz)
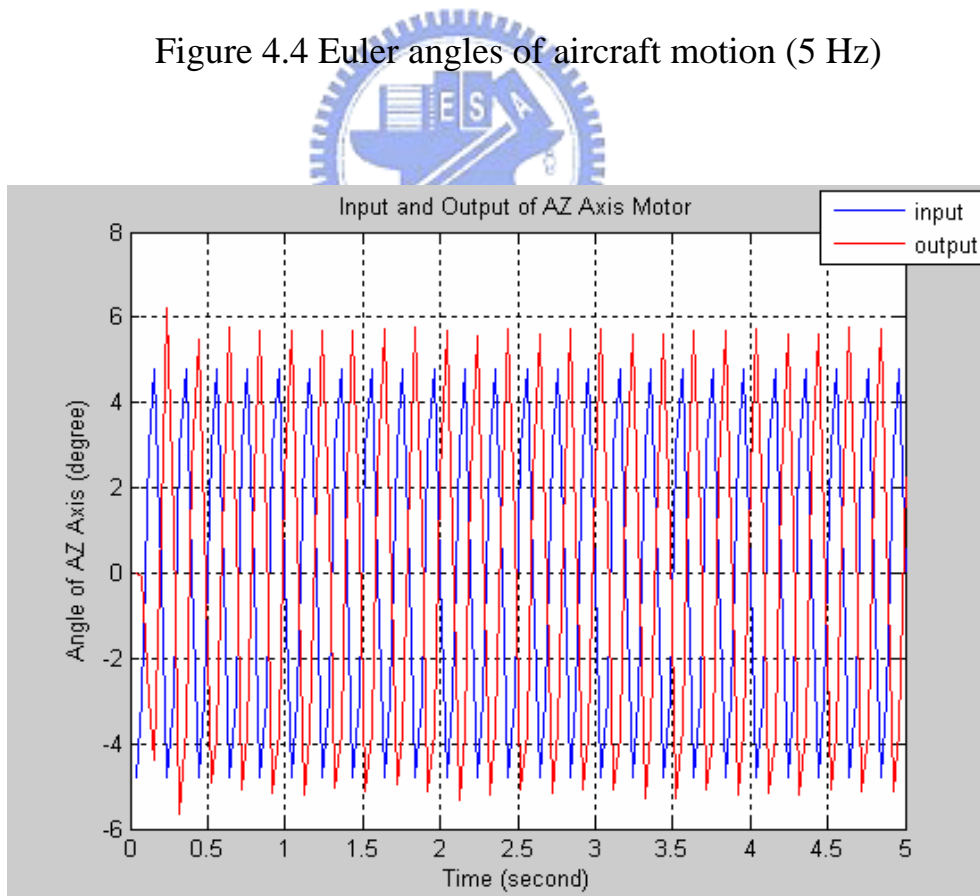
Figure 4.5 AZ axis input and output (5 Hz)
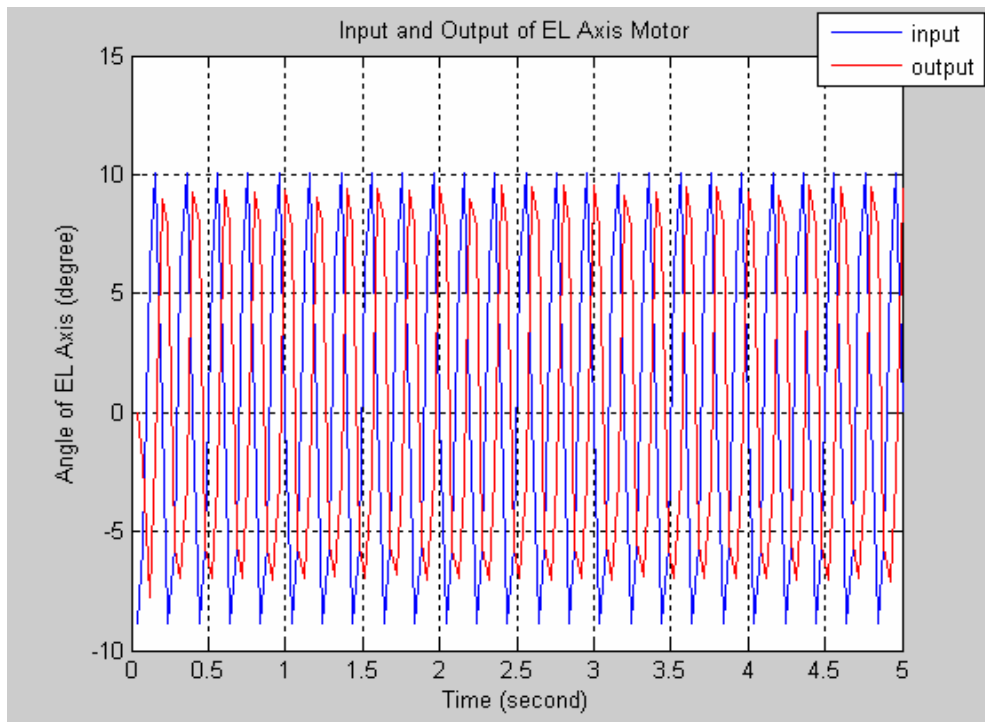
Figure 4.6 EL axis input and output (5 Hz)
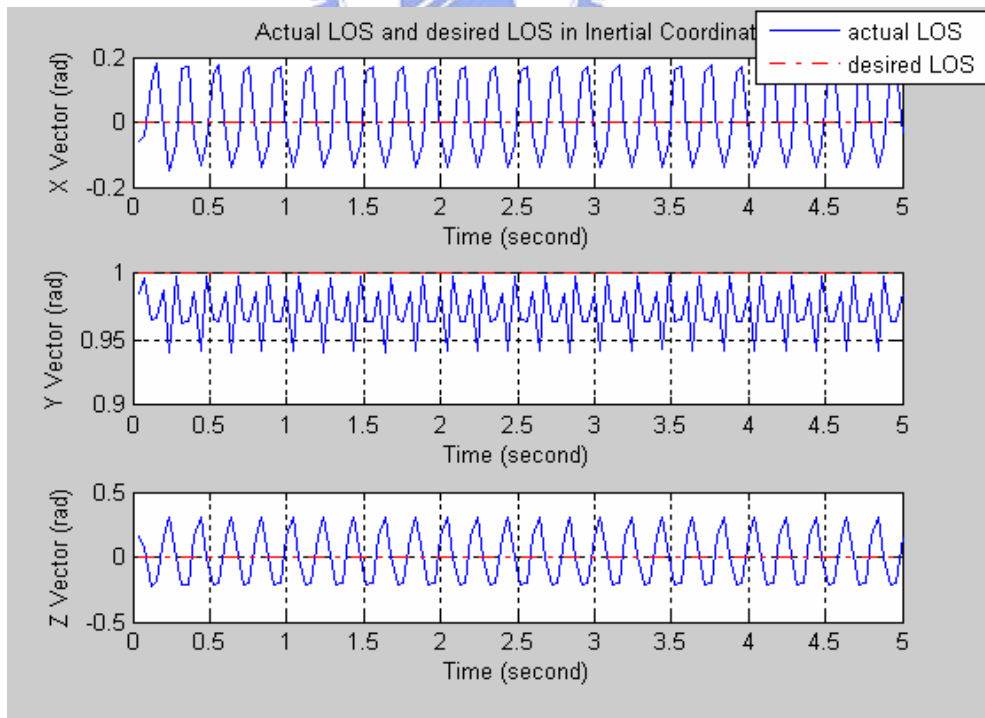
Figure 4.7 Function plot of LOS in the inertial coordinate (5 Hz)

47
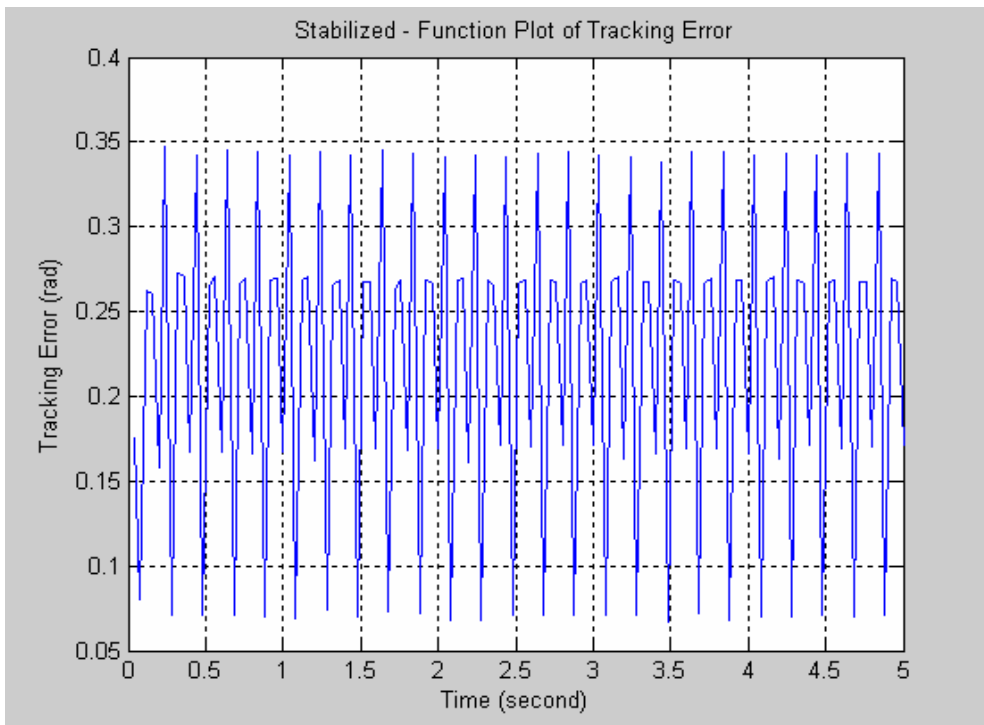
Figure 4.8 Function plot of tracking error (5 Hz)

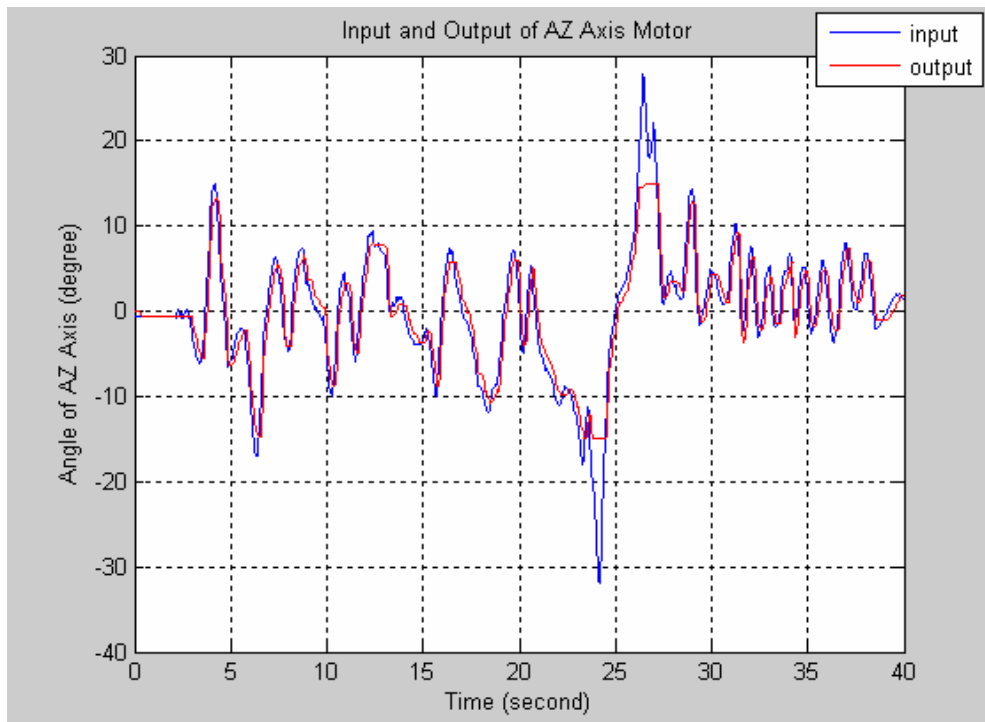Figure 4.9 Euler angles of aircraft motion (random motion)
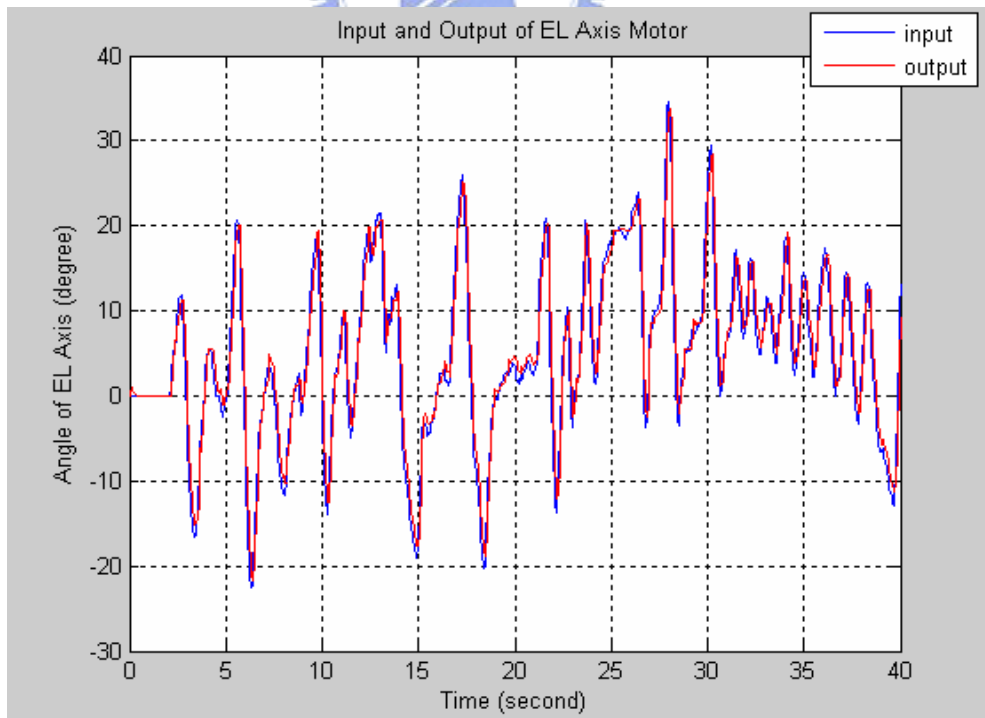
Figure 4.10 AZ axis input and output (random motion)

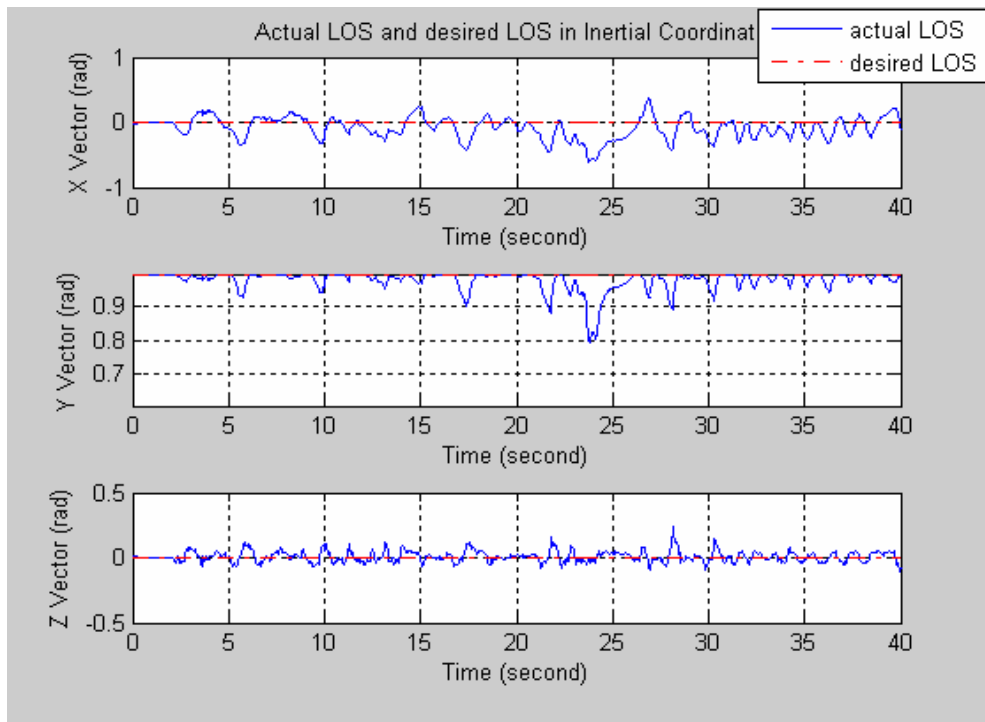Figure 4.11 EL axis input and output (random motion)

49

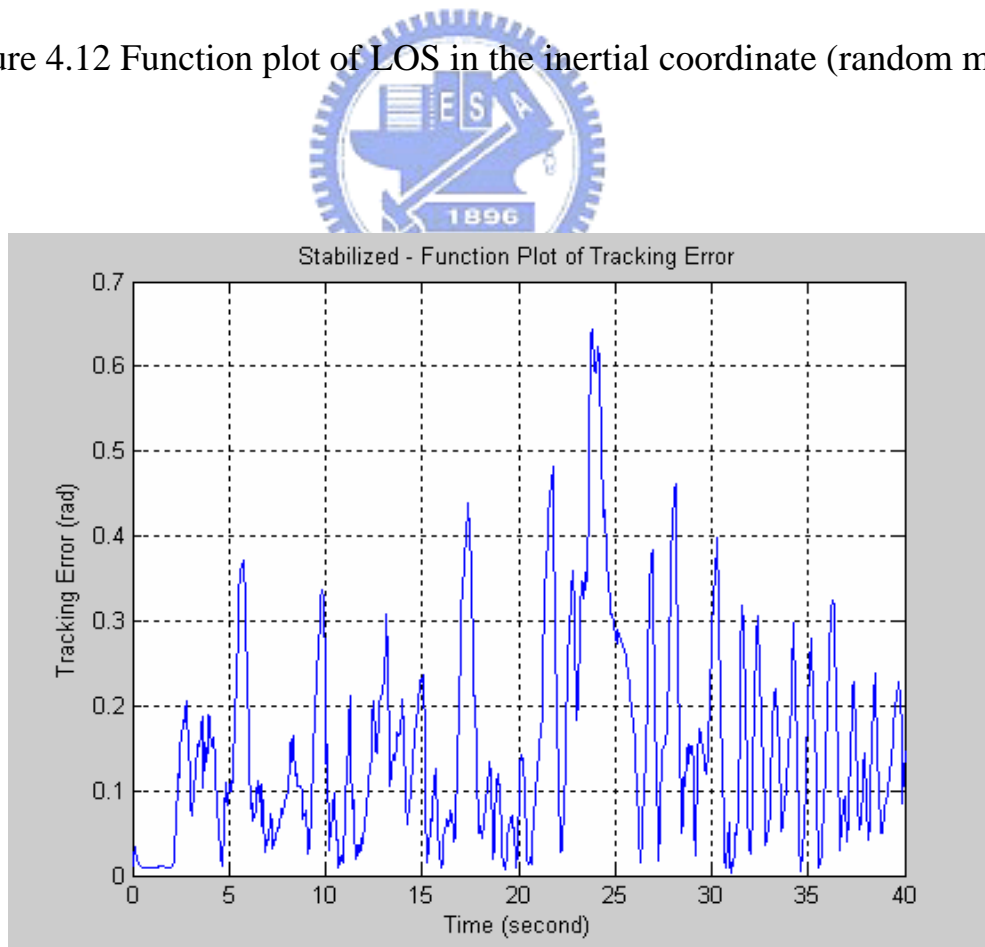Figure 4.12 Function plot of LOS in the inertial coordinate (random motion)

Figure 4.13 Function plot of tracking error (random motion)

Tables

Control	Proportional Gain K_P	Integral Time T_I	Derivative Time T_D
P	$0.5K_c$		
PI	$0.45K_c$	$0.833T_c$	
PID	$0.6K_c$	$0.5T_c$	$0.125T_c$

Table 4.1 Ziegler-Nichols tuning of PID regulators